Dystroglycan loss disrupts polarity and β-casein induction in mammary epithelial cells by perturbing laminin anchoring

M. Lynn Weir[1], Maria Luisa Oppizzi[1], Michael D. Henry[2], Akiko Onishi[1], Kevin P. Campbell[2], Mina J. Bissell[3], John L. Muschler[1]

[1]California Pacific Medical Center Research Institute, San Francisco, CA 94107
[2]Howard Hughes Medical Institute, Dept. of Physiology and Biophysics, University of Iowa College of Medicine, Iowa City, IA 52242
[3]Division of Life Sciences, Lawrence Berkeley National Laboratory, Berkeley, CA 94720

Condensed title: Dystroglycan mediates laminin anchoring

Key words: dystroglycan, laminin, polarity, mammary, epithelial, integrin

# of words: 7,900

Address correspondence to:
Dr. John Muschler
California Pacific Medical Center Research Institute
475 Brannan St., Suite 217
San Francisco, CA 94107

Tel. #: 415-600-1183
Fax #: 415-600-1725
E-mail: Muschler@cpmcri.org

Summary

Precise contact between epithelial cells and their underlying basement membrane is critical to the maintenance of tissue architecture and function. To understand the role that the laminin receptor dystroglycan (DG) plays in these processes, we assayed cell responses to laminin-111 following conditional ablation of DG expression in cultured mammary epithelial cells (MECs). Strikingly, DG loss disrupted laminin-111-induced polarity and β-casein production, and abolished laminin assembly at the step of laminin binding to the cell surface. DG re-expression restored these deficiencies. Investigations of mechanism revealed that DG cytoplasmic sequences were not necessary for laminin assembly and signaling, and only when the entire mucin domain of extracellular DG was deleted did laminin assembly not occur. These results demonstrate that DG is essential as a laminin-111 co-receptor in MECs that functions by mediating laminin anchoring to the cell surface, a process that allows laminin polymerization, tissue polarity, and β-casein induction. The observed loss of laminin-111 assembly and signaling in DG-/- MECs provides insights into the signaling changes occurring in breast carcinomas and other cancers, where DG's laminin-binding function is frequently defective.

Introduction

Laminins are important structural and signaling components of basement membranes (BMs), serving as critical modulators of BM assembly, cellular architecture, and tissue morphogenesis and function (Miner and Yurchenco, 2004). Interaction of laminins with epithelial cells influences such cellular responses as adhesion, polarity, and survival (Li et al., 2003). Genetic defects in laminin subunits result in muscular dystrophies and skin blistering (Miner and Yurchenco, 2004) and disregulated cell-laminin interactions have been implicated in the progression of cancers (Patarroyo et al., 2002). We are using the mammary gland as a model system for understanding cellular interactions with laminins that regulate signals for epithelial architecture and function. Laminin-111 [(previously named laminin-1(Aumailley et al., 2005)] is a key player in these processes in mammary epithelial cells (MECs), inducing polarization (Gudjonsson et al., 2002; Slade et al., 1999) and β-casein production (Streuli et al., 1995). The identities of the multiple laminin receptors which elicit these effects are not completely understood, nor are the cooperative relationships among these receptors. Thus far, the integrins have been implicated (Muschler et al., 1999; Slade et al., 1999; Streuli et al., 1991; Weaver et al., 1997) and, based on indirect evidence, we have postulated an important role for dystroglycan (Weir and Muschler, 2003).

Dystroglycan (DG) is a heterodimeric glycoprotein encoded by a single gene (*DAG1*) and is located on cell surfaces in most adult tissues (Michele and Campbell, 2003). It consists of a transmembrane β-subunit of 43 kDa and a non-covalently associated, extracellular α-subunit of 120-200 kDa (Fig. 1A). The cytoplasmic domain possess known signaling motif and links to the actin cytoskeleton, while the extracellular domain is capable of interacting with extracellular matrix (ECM) proteins, such as laminins, agrin, and perlecan (Michele and Campbell, 2003). Binding of DG to laminin-111 occurs at the C-terminal globular domains (LG4 -5) of the laminin α subunit (Ervasti and Campbell, 1993; Gee et al., 1993) (Fig. 1B). In skeletal muscle, DG serves as a transmembrane link between laminin-2 in the ECM and the intracellular actin cytoskeleton, possibly stabilizing the muscle cell membrane (Ervasti and Campbell, 1993). In such cells, DG forms part of the dystrophin-glycoprotein complex, and certain defects in these components result in distinct muscular dystrophies (Durbeej and Campbell, 2002).

In some tissues, DG has been shown to play a role in BM formation. Knockout of DG in mice is embryonic lethal, resulting in a lack of laminin recruitment and formational defects in Reichert's membrane, an extra-embryonic BM (Williamson et al., 1997). In DG-/- mouse embryoid bodies, disruption of the BM was seen with an almost total loss in laminin cell surface binding (Henry and Campbell, 1998). In a skeletal muscle cell line, laminin-111 and laminin-211 polymerized while interacting with DG and integrins on the cell surface, suggesting a model for receptor-facilitated self assembly of laminins (Colognato et al., 1999).

Several studies have implicated DG in BM-induced epithelial functions, consistent with its location on the basolateral surface of epithelial cells contacting the BM, including those in the mammary gland (Durbeej et al., 1998). Based on antibody perturbation studies, DG plays a role in epithelial morphogenesis in kidney, lung, and salivary gland (Durbeej et al., 1995; Durbeej et al., 2001). Genetic disruption of dystroglycan expression revealed functions in survival of Drosophila epithelial cells (Deng et al., 2003)

and epiblasts of embryoid bodies (Li et al., 2002). DG has been implicated also in epithelial polarity by the study in Drosophila (Deng et al., 2003) and by over-expression in a tumorigenic human MEC line (Muschler et al., 2002).

Since DG knockout in mice is embryonic lethal (Williamson et al., 1997), DG functions have not been assessed by genetic means in adult mammalian epithelial cells. Here we have used a genetic approach in cultured cells to investigate DG's contribution to laminin-111-induced epithelial architecture and function. We examined the effect of a DG gene deletion on laminin assembly and laminin-111-induced responses in adult mouse MEC lines. Results presented here demonstrate for the first time that DG serves as a critical MEC co-receptor mediating cell responses to the basement membrane that include epithelial polarization and β-casein induction. We also dissect the critical receptor domains and demonstrate that DG enacts these signals by anchoring laminin-111 to the cell surface, thereby facilitating laminin-111 polymerization and subsequent signaling.

Materials and methods

Production of immortalized floxed DG mouse MEpG and MEpL cell lines

Mammary glands from homozygous floxed DG transgenic mice (Moore et al., 2002) were digested at 37°C in 0.2% trypsin (Invitrogen), 0.2% collagenase A (Roche), DME/F12 (HyClone), 5% FBS (HyClone), 5 μg/mL insulin (Sigma), and 50 μg/mL gentamicin (Invitrogen), followed by centrifugation (400xg, 5 s) until fibroblast-free. Cells were grown in plastic flasks (MEpG cell line) or collagen I gels (Cellagen; ICN Biomedicals) (Kittrell et al., 1992) for 5 weeks prior to collagenase A digestion of the gel and cell transfer to plastic flasks (MEpL cell line). Cells were grown in DME/F12, 2% FBS, 10 μg/mL insulin, 5 ng/mL EGF (BD Biosciences), and 50 μg/mL gentamicin (=complete media) in humidified 5% CO_2 at 37°C and passaged using dispase II (Roche) until spontaneously immortalized, after which 0.025% trypsin/0.27 mM EDTA (Cellgro) were used. Clones were obtained by limiting dilution and screened for expression of epithelial markers by immunofluorescent staining.

Generation of DG+/+ and partial DG-/- mouse MEC populations

Adenoviral vectors (Microbix) were amplified twice in QBI-293 packaging cells (Quantum Biotechnologies), grown in DMEM (Invitrogen), 2 mM Gln, 10% FBS, and 10 μg/mL gentamicin. Immortalized floxed DG mouse MEC lines (MEpG, MEpL) were infected with either control (Ad.flox*lacZ*1) or Cre recombinase-expressing (Ad.*cre*M1) adenoviral supernatants with multiplicity of infection of 40-50.

Expression of full length DG and mutants in completely DG-/- MEC lines

Human DG coding sequence was subcloned from pLXSN vector (Muschler et al., 2002) into the EcoRI site of the retroviral expression vector, pBMN-IRES-PURO (Kinoshita et al., 1997). From this construct, β-DG cytoplasmic deletion mutants were constructed using the QuikChange XL Site-Directed Mutagenesis Kit (Stratagene) and verified by sequencing. DEL A, B, C, D, and E lacked amino acids 780-895, 806-880, and 881-895, 315-485, and 400-485, respectively (Fig. S3). DG-tmf was constructed from the ligation of 2 PCR products spanning amino acids 1-739 of DG, and amino acids 656-699 of the human TACE gene. The reverse primer for the TACE PCR product included the coding sequence for 10 aditional amino acids at the C-terminus (LDEESILKQE), representing the Myc tag. Retrovirus was generated using Phoenix-ECO packaging cells grown in DME/H21 (UCSF Cell Culture Facility) and 10% FBS and transfected using calcium phosphate (Sambrook et al., 1989).

DG-/- clones were obtained by limiting dilution of partial DG-/- MEC populations and screened by immunostaining for lack of DG expression. Clones were seeded in 100 mm dishes, infected with 2 mL of retroviral supernatant, 6 mL of complete media, and 8 μg/mL polybrene, and selected in complete media with 5-10 μg/mL puromycin (Sigma).

3-D polarity assays

Trypsinized cells (~10^4 - 10^5) were added to 300 uL of collagen I (Cellagen; ICN Biomedicals) or collagen I/laminin-111 (35 μg; Sigma) on ice. Matrices were solidified at 37°C and covered with complete media with changes every 2 d. On d 6 or 7, samples were immunostained. For polarity quantification, colonies with >3 nuclei were considered polar if ZO-1 staining was centrally located within the colony. For statistical

analysis, comparisons between groups were subject to one way analysis of variance and differences between means were determined using Fisher's least significant difference method.

β-casein and laminin assembly assays

β-casein assays were performed as previously described (Muschler et al., 1999), except that 5 μg/mL prolactin and serum-free complete media were used. To assess laminin assembly, laminin-111-FITC was prepared by dialysing laminin-111 (Sigma) in PBS, 10 μM $CaCl_2$, and incubating with NHS-fluorescein (Pierce) for 2 h at 4°C in the dark. Dialysis was repeated, and laminin-111-FITC was measured by the Lowry protein assay (Peterson, 1977). Laminin-111 was treated with AEBSF (Calbiochem) as described (Colognato et al., 1999). Cells grown on Lab-Tek II CC2 glass chamber slides (Nalge Nunc) were immunostained following incubation at 37°C in the dark in serum-free complete media with 10 nM AEBSF-treated laminin-111 for 24 h or 10 nM laminin-111-FITC for 4 or 24 h (latter with or without integrin function-blocking antibodies).

Immunofluorescent staining

Cells grown on Lab-Tek II CC2 glass chamber slides (Nalge Nunc) or in 3-D polarity assays were washed twice in PBS. Some 3-D samples were digested with 0.2% collagenase A in complete media at 37°C to remove matrix for easier counting. For actin/α6 integrin, DG, and laminin staining, samples were fixed in 2% formaldehyde in PBS for 10 min, RT and washed in PBS, 25 mM glycine for 3x10 min. For ZO-1/α6 integrin staining, samples were fixed in acetone/methanol (1:1) at -20°C for 5 min and air-dried. After blocking in PBS, 10% goat serum (Sigma), 0.1% Tween-20 for 1 h, RT, samples were incubated in blocking solution overnight at 4°C with primary antibodies, followed by 1 h, RT with fluorescent secondary antibodies. For actin staining, Alexa Fluor 488 phalloidin (Molecular Probes) was used for 20 min, RT using 1:21 dilution in blocking solution. Nuclei were counterstained with 10 μg/mL propidium iodide (Sigma). Washes between antibody incubations were 3x10 min in PBS. Samples were mounted in Vectashield mounting media (Vector Laboratories) with glass coverslips.

Microscopy

Immunofluorescent images were obtained with a Nikon Eclipse TE2000-U inverted microscope, Photometrics CoolSNAP HQ camera, MetaMorph 6.1r1 software (Universal Imaging Corporation), and a Nikon Plan Ph1 DL 20X objective (0.40 NA) (Fig. 4C inset obtained with Nikon Plan Apo DIC H 60X oil objective of 1.40 NA). Confocal images were obtained with the same microscope and a Nikon D-Eclipse C1 confocal attachment, Nikon EZ-C1 2.10 software, channel series setup, and the 60X oil objective. Images were cropped and adjusted for contrast using Adobe Photoshop 7.

Western blots

Cell extracts were prepared in 62.6 mM Tris-HCl, pH 6.8, 2% SDS, 5% glycerol, 5 μg/mL pepstatin (Sigma), 500 μM AEBSF, 150 nM aprotinin, 1 μM E-64, 0.5 mM EDTA, 1 μM leupeptin (all from Calbiochem) and measured using the Lowry protein assay (Peterson, 1977). SDS-PAGE was performed under reducing conditions using equal amounts of protein and 4-12% or 4-20% polyacrylamide Tris-glycine gradient gels.

Proteins were electrophoretically transferred to Immobilon-P membranes (Millipore). Blots were blocked in 5% non-fat dry milk in TBS-T (50 mM Tris-HCl, pH 7.4, 100 mM NaCl, 0.1% Tween-20) for 1 h, RT, followed by incubation in blocking buffer overnight at 4°C with primary antibodies, then 1 h, RT with HRP-conjugated secondary antibodies.. Blots were washed in TBS-T after antibody incubations, and bands were visualized with the ECL/ECL Plus systems (Amersham Pharmacia).

Antibodies

Mouse mAbs specific for C-terminal β-DG (NCL-b-DG; Novocastra), N-terminal β-DG (BD Biosciences), E-cadherin (BD Transduction Labs), and β-casein (Kaetzel and Ray, 1984) were used for immunoblotting at 1:200, 1:500, 1:5000, and 1:2000, respectively. The former antibody was used for immunostaining at 1:50. Rabbit pAbs specific for ZO-1 (Zymed) or laminin purified from the BM of Engelbreth-Holm-Swarm mouse sarcoma (Sigma) were used for immunostaining at 1:100 and 1:40, respectively. Rat mAb GoH3 specific for α6 integrin (Chemicon) was used for immunostaining at 1:30. Mouse IgM mAb IIH6C4 specific for α-DG (Ervasti and Campbell, 1991) (Upstate, Inc.) was used for immunostaining at 1:200 and immunoblotting at 1:300. Function blocking antibodies for α6 and β1 integrins were used at 10 and 50 μg/mL, respectively (PharMingen). The anti-α6 antibody was later tested at 100 μg/ml, and produced the same result.

Cy-5-, FITC-, or rhodamine-conjugated, affinity-absorbed antibodies specific for mouse, rat, or rabbit IgG and mouse IgM (Amersham Pharmacia; Chemicon; Caltag) were used at a 1:50 dilution. HRP-conjugated antibodies specific for mouse IgG (Amersham Pharmacia) and mouse IgM (Sigma) were used for Western blots at 1:2000 and 1:3000, respectively.

Online supplemental material

Fig. S1. Established cell lines display epithelial markers before and after adenoviral infection. Monolayers of uninfected MEpG cells (left panel) or those infected with either a control or Cre-expressing adenovirus to generate DG+/+ cells (middle panel) or DG-/- cells (right panel), respectively, were fixed in acetone/methanol and immunostained as described in Materials and methods. Mouse mAb specific for E-cadherin (BD Transduction Labs) was used at 1:200. Rat mAb TROMA-1 specific for keratin 8 was used at 1:30 (obtained from Developmental Studies Hybridoma Bank under the auspices of the NICHD; maintained by University of Iowa, Dept. of Biol. Sciences, Iowa City, IA) (Kemler et al., 1981). Both of the former antibodies were visualized with FITC-conjugated secondary antibodies (green). Rabbit pAb specific for ZO-1 (Zymed) was used at 1:100 and detected with rhodamine-conjugated secondary antibody (red). Images were captured using a Nikon Eclipse E800 microscope, SPOT camera (Diagnostic Instruments Inc), Image-Pro Plus 3.0.01.00 software (Media Cybernetics), and a Nikon Plan Fluor Ph1 DLL 20X objective (0.50 NA). Bar, 60 μm.

Fig. S2. DG protein levels in DG+/+ and partial DG-/- MEC populations generated by adenoviral infection of the MEpL cell line. Shown in A is a Western blot of cell extracts (10 μg protein) prepared on various days after infection of immortalized floxed DG mouse MEpL cell line with control or Cre recombinase-expressing adenovirus to generate DG+/+ or partial DG-/- cell populations, respectively. Lane 1 represents uninfected cells at time 0. Antibodies are described in the legend for Fig. 1. Sizes of

molecular weight markers are given in kDa. Shown in B are vertically paired immunofluorescent images of DG+/+ and partial DG-/- cell populations that were stained using a C-terminal β-DG antibody followed by a FITC-labeled secondary antibody (upper panel). Nuclei were stained with propidium iodide (bottom panel). Bar, 60 μm.

Fig. S3. Diagram of DG mutants. Shown are the structures of full length DG (wtDG), deletion mutants (DEL A, B, C, D, and E) and the transmembrane fusion mutant (DG-tmf), consisting of extracellular DG sequences fused to the transmembrane domain of TACE. Numbers refer to amino acids in human α- and β-DG, with deleted sequences shown by dotted lines. "PM" refers to the plasma membrane."TM" refers to the transmembrane domain of β-DG, and "tm" to the transmembrane domain of TACE.

Results

Establishment of DG+/+ and partial DG-/- mouse MEC populations

In order to assess DG function in adult mouse MECs, a culture system was developed in which DG gene expression could be conditionally abrogated using Cre-*lox* recombination. We established two spontaneously immortalized MEC lines, MEpG and MEpL (*M*ammary *Ep*ithelial clones *G* and *L*), from mammary glands of floxed DG transgenic mice (see Materials and Methods). Infection of these cells with Cre recombinase-expressing adenovirus resulted in recombination between *loxP* sites flanking exon 2 of the DG gene, subsequent DG gene inactivation, and creation of DG-/- MECs.

Both MEpG and MEpL cell lines were epithelial in nature, as judged by tightly packed, cobblestone-like morphologies and expression of typical MEC markers; immunodetection revealed expression of epithelial ZO-1, E-cadherin, and keratin 8 (Fig. S1, left panel), but not myoepithelial α-smooth muscle actin or vimentin (data not shown). The MEpG cell line was used for laminin assembly and polarity assays; these cells did not express β-casein. The MEpL cell line was used for laminin assembly and β-casein assays, but not for polarity analyses. Many MEpL colonies produced pseudopod-like extensions when grown in 3-D matrices, making assessment of polarization difficult.

Infection of the MEpG cell line with control adenovirus produced a control DG+/+ cell population which retained expression of DG protein over time, as shown by Western blotting (Fig. 1C) and immunostaining (Fig. 1D) for α- and β-DG. Parallel infection of the MEpG cell line with Cre recombinase-expressing adenovirus, to produce a DG-/- cell population, resulted in a near complete loss of DG protein expression, as demonstrated by Western blotting for α- and β-DG (Fig. 1C). Immunostaining revealed that about 90% of the Cre-infected MECs lacked α- and β-DG expression (Fig. 1D). Similar results were obtained upon adenoviral infection of the MEpL cell line (Fig. S2). DG+/+ and partial DG-/- cell populations retained the epithelial marker expression profile seen in MEpG and MEpL parent cell lines prior to adenoviral exposure, showing that neither viral infection nor DG loss altered the epithelial phenotype (Fig. S1 and data not shown).

DG loss and MEC polarity

To investigate the role of DG in laminin-111-induced MEC polarization, DG+/+ and partial DG-/- cell populations were grown in 3-D matrices containing collagen-1 with or without laminin-111, established culture models that can mimic the in vivo MEC response to the BM microenvironment. Polarity was assessed by examining the distribution of ZO-1, α6 integrin, nuclei, and cytoskeletal actin.

Immunofluorescent staining of DG+/+ and DG-/- colonies grown in collagen I revealed a random distribution of nuclei, ZO-1 and α6 integrin (Fig. 2A, upper panel). Actin and DG (latter in DG+/+ cells only) showed apolar patterns similar to α6 integrin (Fig. 2B, upper panel). Quantification of polarization using ZO-1 staining revealed few polar DG+/+ or DG-/- colonies in collagen I (Fig. 2C).

When laminin-111, a known inducer of polarization of mammary gland acini, was added to the collagen I matrix, DG+/+ cells polarized, displaying dramatic changes in the

distribution of polarity markers and the cytoskeleton (bottom left images in Fig. 2A, B). ZO-1 and actin were found at the center of colonies, consistent with apical formation of tight junctions and an underlying cytoplasmic actin belt. DG and α6 integrin were localized basolaterally on cell surfaces and nuclei shifted to the colony periphery. Quantification using ZO-1 staining revealed a significant increase in polarized colonies in collagen I/laminin-111 compared to collagen I alone (35.3% vs. 8.0%, $P<0.01$; Fig. 2C).

Unlike DG+/+ cells, DG-/- cells did not significantly polarize in collagen I/laminin-111 (bottom right images in Fig. 2A, B), exhibiting polarization levels similar to those seen in collagen I (Fig. 2C). Increasing laminin-111 from 35 to 75 μg in the collagen matrix did not elevate polarization of DG+/+ or DG-/- cells further (data not shown). The inability of DG-/- cells to polarize in response to laminin-111 was not due to a problem in tight junction formation, since ZO-1 still localized at cell-cell contacts in confluent monolayers of DG-/- cells grown on plastic (Fig. S1, right middle panel).

DG links laminin assembly and MEC polarity

DG has been implicated in laminin assembly in a few cell types (Colognato et al., 1999; Henry and Campbell, 1998; Williamson et al., 1997), but such a role in differentiated epithelial cells has not been investigated. To test the hypothesis that DG-/- MECs failed to polarize in response to laminin-111 because of laminin assembly defects, DG+/+ and DG-/- cells in 3-D polarity assays were immunostained using a polyclonal antibody raised against laminin-111 subunits.

Apolar DG+/+ cells in collagen I showed punctate patterns, small patches, and polygonal arrays of endogenously produced laminin on colonies' outer surfaces (Fig. 3A, left of top panel), which co-localized with DG in many regions (Fig. 3B, top panel). Apolar DG-/- cells in collagen I lacked laminin surface staining (Fig. 3A, right of top panel). Importantly, in collagen I/laminin-111 gels, polarized DG+/+ cells had an extensive laminin network on colonies' outer surfaces (Fig. 3A, left of 3rd panel), which co-localized with DG as a more continuous polygonal array than seen in collagen I alone (Fig. 3B, bottom panel). In contrast, apolar DG-/- cells in collagen I/laminin-111 were deficient in laminin surface staining (Fig. 3A, right of 3rd panel).

In order to determine if the observed lack of laminin staining on DG-/- cells was unique to the 3-D ECM environment, laminin assembly was examined further using cell monolayers. Staining of DG+/+ cells for endogenous laminin revealed a diffuse, intracellular component and a punctate, extracellular pattern (Fig. 4A, left images above line). In contrast, cells lacking DG in the partial DG-/- cell population exhibited intracellular, but not extracellular, laminin staining (Fig. 4A, right images above line). Laminin locations were confirmed by using unpermeabilized cells where only extracellular laminin staining was visible due to lack of intracellular access by the anti-laminin antibody (Fig. 4A, images below line).

To observe the assembly of laminin-111 exclusively, cells were exposed to exogenous laminin-111-FITC for 4 h and imaged without the use of antibodies. Examination of DG+/+ cell monolayers revealed punctate patterns and extensive patches of surface laminin-111-FITC (Fig. 4B, left panel). This binding was found to be time- and concentration-dependent with initial punctate patterns evolving into progressively larger, connected patches (data not shown). In contrast, cells lacking DG in the partial DG-/-

cell population did not show laminin binding at any time (4-24 h) or even at a high concentration of 10 nM laminin-111-FITC (Fig. 4B, right panel; data not shown).

These findings demonstrate that DG-/- cells retain the ability to synthesize laminin, but are unable to bind endogenous laminins or exogenous laminin-111 either in monolayers or within a 3-D matrix. Hence, DG serves as the critical link between laminin-111 interaction with MECs and subsequent induction of polarization in a 3-D environment.

To test whether DG and integrins cooperate in laminin assembly in MECs, we employed integrin function-blocking antibodies. DG+/+ cells were exposed to laminin-111-FITC for 24 h, a time at which extensive polymerization had occurred (Fig. 4C, left panel). Blocking of α6 integrins had no effect on laminin-111 assembly (Fig. 4C, 2nd panel from left). However, inhibition of β1 integrins severely diminished the extent of laminin-111 polymerization, but still allowed laminin cell-surface binding (Fig. 4C, 3rd panel from left). This pattern was similar to that seen when DG+/+ cells were incubated with non-polymerizing laminin-111 and immunostained for laminin (Fig. 4C, insets in 3rd panel from left). This laminin was generated by treatment with p-aminoethylbenzenesulfonyl fluoride (AEBSF) (Colognato et al., 1999). Inclusion of both α6 and β1 integrin blocking antibodies produced a result similar to that seen with the β1 antibody alone (Fig. 4C, right panel). These findings show that DG and β1 integrins cooperate in laminin-111 assembly on MECs, with DG serving as the initial binding site enabling β1 integrins to participate in subsequent polymerization and signaling.

Chimeric MEC colonies do not polarize

Cues for epithelial polarization originate from the BM and neighboring cells (Yeaman et al., 1999). To determine whether DG influences polarization of neighboring cells and the minimal number of DG expressors required for colony polarization, we analyzed the polarity of chimeric colonies containing both DG+/+ and DG-/- cells. Such colonies were produced in polarity assays using the partial DG-/- MEpG population, which contained a subpopulation of DG+/+ cells (Fig. 1). Staining of chimeric colonies in collagen I/laminin-111 for actin and α6 integrin revealed an apolar phenotype, even when half or more of the cells in the colony were DG+/+ (Fig. 5A). Quantification using α6 integrin staining showed minimal levels of overall polarization in chimeric colonies even when the majority of cells in a colony were DG expressing (avg.$\pm$std.dev.= 0.98$\pm$1.34%; n=5 counts x 40 colonies per count). Interestingly, laminin staining was visible only on the surface of DG+/+ cells, where it co-localized with DG in an extensive reticular network (Fig. 5B, C). These observations suggest that global DG expression in MEC colonies is essential in order for laminin-111 to assemble around the entire colony and trigger cooperative participation of all cells in colony polarization.

DG loss disrupts β-casein production in MECs

Previous results indicated that BM-induced β-casein expression in MECs required β1 integrins, α6β4 integrin, and a laminin receptor binding the LG4-5 domains (Faraldo et al., 1998; Muschler et al., 1999; Streuli et al., 1991). To determine directly the role of DG in laminin-111-induced β-casein production, DG+/+ and partial DG-/- MEC populations (derived from the MEpL cell line) were tested in β-casein assays using lactogenic hormones and a laminin-111 overlay (Streuli et al., 1995).

DG+/+ and the partial DG-/- cell populations produced β-casein protein in response to laminin-111 in the presence, but not absence, of lactogenic hormones, as expected (Fig. 6A). However, the partial DG-/- cell population showed a drastic reduction in laminin-111-induced β-casein levels. As expected, no β-casein was detected in either cell population upon omission of the laminin-111 overlay (Fig. 6A).

Analysis of the ability of DG+/+ and partial DG-/- cells to bind laminin revealed results similar to those seen with the MEpG cell line (Fig. 4). DG+/+, but not DG-/-, cell monolayers bound endogenous laminins (data not shown) and exogenous laminin-111-FITC (Fig. 6B). These results show that the decrease in laminin-111-induced β-casein levels in the partial DG-/- cell population is due to disruption of laminin-111 binding to DG-/- cells.

The DG extracellular domain alone is critical to laminin assembly.

The β-subunit of DG contains cytoplasmic sites potentially recognized by SH3, SH2, and WW domain proteins (Ibraghimov-Beskrovnaya et al., 1992; Pawson, 2004). To investigate whether DG plays an active signaling role in MEC functions, three β-DG cytoplasmic domain deletions were generated and tested (Fig. S3). DEL A lacked the entire cytoplasmic domain, except for six amino acids beyond the transmembrane region. DEL B had an internal deletion resulting in retention of the C-terminal 15 amino acids and proximal removal of several potential WW, SH3, and SH2 domain protein recognition sites. DEL C lacked the C-terminal 15 amino acids, which contain proven interaction sites for SH3, SH2, and WW domain proteins (Ilsley et al., 2002; Sotgia et al., 2001; Yang et al., 1995).

We generated a completely DG-/- cell line by single cell cloning from the partially DG-/- MEpG cell population and then infected the DG-/- cell line with either empty retroviral vector (VEC) or vector encoding full length DG (wtDG), DEL A, DEL B, or DEL C. Western blots showed that VEC cells were deficient in α- and β-DG protein (Fig. 7A, left panels), whereas the other infected cells expressed α-DG of the same size as in DG+/+ cells (Fig. 7A, upper left panel). An N-terminal β-DG antibody verified expression of the full length β-subunit in wtDG cells and truncated versions in DG mutant cells (Fig. 7A, upper right panel). A β-DG antibody recognizing an epitope in the C-terminal 15 amino acids detected the β-subunit in wtDG and DEL B cells, but not in DEL A or C cells, verifying the lack of this epitope in the latter two populations (Fig. 7A, middle left panel).

α-DG was correctly localized to the surface of wtDG and DG mutant cells and was not detected on VEC cells (Fig. 7B). Laminin-111-FITC bound and assembled at the surface of wtDG, but not VEC, cells, showing that DG re-expression corrected the laminin assembly defects (Fig. 7C). All DG mutant cells also assembled cell surface laminin-111-FITC comparable to wtDG cells, revealing, surprisingly, that DG cytoplasmic domains were not required (Fig. 7C). Identical results were obtained upon expressing wtDG or DG mutants in DG-/- cells derived from the MEpL cell line (data not shown).

Analysis of laminin-111-induced polarity in VEC, wtDG, and DG mutant cells demonstrated very few polar colonies in collagen I (Fig. 8A, top panel; 8B). Addition of laminin-111 to the collagen I gel resulted in significant increases in the number of polar colonies for all but the DG-/- (VEC) cells (Fig. 8A, middle panel; 8B). In addition, immunostaining revealed laminin localization on colony surfaces of all but VEC cells grown in collagen I/laminin-111 (Fig. 8A, bottom panel). Likewise, laminin-111-induced

β-casein levels were restored in wtDG and DG mutant cells compared to VEC cells (Fig. 9). However, even in the complete absence of DG expression, low levels of β-casein were seen in VEC cells treated with laminin-111. As in Fig. 6A, no β-casein was detected in any of the cell populations in the absence of a BM overlay.

Additional DG mutants were created to investigate the role of DG transmembrane and extracellular domain sequences in laminin assembly (Figure S3). The DG cytoplasmic and transmembrane domains were replaced by 44 amino acids encompassing the transmembrane domain of the "TNF-α cleaving enzyme" (TACE) (Moss et al., 1997), plus an unrelated 10 amino acid cytoplasmic tail. When expressed in the DG-/- MEpL cells, this fusion protein (DG-tmf) permitted laminin anchoring and assembly (Fig. 10). A mutant possessing a large deletion in the C-terminal half of the mucin domain (DEL E) also functioned like the wild-type protein. Importantly, only expression of a DG cDNA lacking the entire mucin domain (DEL D) failed to bind and assemble laminin (Fig. 10).

Discussion

Laminins are key signaling modulators of cellular architecture and function during embryonic and post-natal development (Li et al., 2003; Miner and Yurchenco, 2004). In mammary epithelial cells, laminin-111 interaction with cell surface receptors is important for induction and retention of differentiated features, including cellular and tissue polarity and β-casein expression (Gudjonsson et al., 2002; Slade et al., 1999; Streuli et al., 1995). Using a DG genetic deletion in adult MEC lines, we show here that DG plays a crucial role as a laminin-111 co-receptor in MEC functions, acting at an initial and critical step (see model, Fig. 11). We demonstrate that DG mediates laminin-111 anchoring to the MEC surface, such that subsequent laminin-111 polymerization and induction of signals linked to polarity and β-casein levels can proceed via other co-receptors.

Role of DG in laminin assembly

Although most laminins self-assemble spontaneously, the process is facilitated by interaction with cell surface receptors. This mechanism involves receptor binding of monomeric laminin via its C-terminal G domain and laminin polymerization via resultant interactions between neighboring N-terminal short arms (Colognato et al., 1999). This polymerization is crucial for recruitment of other BM proteins, cytoskeletal reorganization, and signaling events (Colognato et al., 1999).

Data presented here demonstrate in an adult epithelial cell type (MECs) that DG and β1 integrins cooperate in receptor-facilitated laminin assembly. Significantly, we find that DG is essential for initial laminin-111 binding to MECs such that subsequent polymerization can proceed via β1-integrin co-receptors. These results help to explain BM defects seen upon DG reduction or loss in brain cells, Reichert's membrane, and Drosophila epithelia (Deng et al., 2003; Michele et al., 2002; Moore et al., 2002; Williamson et al., 1997). They also support observations made using embryonic stem cells cultured in monolayer (Henry and Campbell, 1998; Henry et al., 2001b; Lohikangas et al., 2001). However, the requirement for DG in laminin/BM assembly may be tissue-specific. In one study, assays for BM assembly in ES-derived embryoid bodies show no BM defects in DG-/- embryoid bodies, but show a dramatic loss of epiblast cell survival (Li et al., 2002), although another study shows loss of laminin and BM assembly in DG-/-

embryoid bodies produced by a method that did not generate a differentiated epiblast layer (Henry and Campbell, 1998). In addition, normal BMs are observed upon DG loss in skeletal muscle and some embryonic tissues (Cohn et al., 2002; Michele et al., 2002; Williamson et al., 1997). In Schwann cells and fibroblasts, certain sulfated glycolipids can mediate laminin/BM assembly (Li et al., 2005), raising the possibility that DG and sulfated glycolipids may functionally overlap.

Because DG can mediate laminin assembly and signaling in the absence of endogenous transmembrane and cytoplasmic signaling domains, and also function in the presence of a large internal deletion of the extracellular domain, it appears that laminin anchoring to the cell surface is the main, and possibly only, role for DG in the initiation of assembly and signaling. This model is consistent with observations in fibroblasts and Schwann cells showing that laminin binding to cell-surface glycolipids is also sufficient to initate assembly and signaling (Li et al., 2005). Importantly, no exogenous laminin-111 binding was observed at the surface of DG-/- cells, demonstrating that no other molecule compensated for DG's role in laminin anchoring to MECs. This result also suggests that co-receptors, such as the β1 integrins require the interaction of DG with laminin-111 *prior* to recruitment and/or activation. A recent study in intestinal epithelial cells reported direct interaction of DG and β1 integrins by co-immunoprecipitation (Driss et al., 2005), something we have not yet observed in MECs. This same study also reported an enhancement of integrin-laminin-111 interactions that is dependent on DG cytoplasmic sequences, but this observation is inconsistent with our results in MECs, where deletion of DG cytoplasmic sequences did not perturb function.

DG mediates signals for epithelial architecture and function.

Our results show that DG also plays an essential role in mediating laminin-111-induced MEC functions, including tissue architecture and tissue-specific gene expression. DG-/- cells failed to polarize and showed markedly reduced β-casein production because of defects in laminin-111 binding. In addition, our finding that laminin-111/DG signaling pathways linked to polarity and β-casein levels were independent of β-DG cytoplasmic domains suggests that the functional coupling of DG with co-receptors enacts signaling. Candidate co-receptors include α6β4 or β1 integrins that influence polarity (Faraldo et al., 1998; Slade et al., 1999; Weaver et al., 1997) and β-casein levels (Faraldo et al., 1998; Muschler et al., 1999; Streuli et al., 1991). A partial, albeit low, receptor compensation for DG loss was seen in laminin-111-induced β-casein assays, suggesting that, in the presence of high laminin-111 levels, some spontaneous laminin self-assembly may take place, or interaction with a less effective laminin receptor may occur. Whatever the case, DG is still needed as a laminin-111 co-receptor to allow efficient β-casein production.

The results reported here provide a molecular mechanism to explain why overexpression of DG is capable of reverting and normalizing breast tumor cells, and why the functional status of DG correlates strongly with a tumor cells ability to polarize (Muschler et al., 2002). In addition, they explain the observed requirement for multiple MEC receptors in β-casein expression, including a receptor for the laminin LG4-5 domain that is likely to be DG (Muschler et al., 1999; Streuli et al., 1995). The results can also explain the role of DG in establishing Drosophila epithelial polarity (Deng et al., 2003). However, DG knockout in mouse embryoid bodies does not affect polarization of

epiblast cells (Li et al., 2002) demonstrating that DG is not universally required for polarity in mammalian cells. Epiblast differentiation and polarization are affected in mice lacking the laminin α1 LG4-5 modules, hinting at the existence of other receptors for these modules (Scheele et al., 2005).

Our observation that MEC chimeras of DG expressors and non-expressors did not polarize stresses the importance of laminin assembly along the entire basal epithelial surface to establish normal tissue architecture; loss of laminin assembly on even a minority of cells is sufficient to disrupt polarity in the entire acinar structure. This result illustrates the required integration of both cell-cell and cell-BM interactions to establish cellular and tissue polarity (Yeaman et al., 1999). DG-/- cells of chimeric colonies lacked the ability to bind surface laminin-111 and did not receive the necessary external BM cue for activation of intracellular polarity pathways, which include establishing of proper cell-cell junctions. Consequently, with direct contact of DG+/+ cells and DG-/- cells, the defect of the DG-/- cells was dominant. This defect was sufficient to prevent the establishment of polarity in DG+/+ cells, and was propagated throughout the colony.

DG's significance in vivo and in disease

Our findings have important implications for understanding the abnormal behavior of carcinomas of the breast and other tissues. In breast, prostate, and colon cancers, loss in DG detection correlates with tumor progression (Henry et al., 2001a; Sgambato et al., 2003). In many carcinoma cell lines, including those of the breast, DG lacks laminin binding ability due to glycosylation changes and/or proteolytic processing (Losasso et al., 2000; Muschler et al., 2002; Singh et al., 2004). Our results reveal that localized disruption of the DG/laminin-111 link in MECs leads to losses in laminin-111-induced responses important to normal epithelial architecture and function, with impact on neighboring cells as well. Thus, loss of DG function is a plausible and attractive explanation for some of the aberrant cell responses to the BM that are evident in cancer progression.

Acknowledgements
The authors gratefully acknowledge Ken Yamada, Jimmie Fata, Masahiko Itoh and Peter Yurchenco for helpful discussions and Patrick Hardy, Yoko Itahana, Jae-Young Seo, Sara Cohen, Armin Akhavan, and Hui Zhang for expert technical assistance. We thank Garry Nolan and Lee Opresko for providing the pBMN-IRES-PURO vector with modified cloning site and Phoenix-ECO retroviral packaging cells. This work was supported by NIH Grant R01 CA10957-01, and California Breast Cancer Research Program Grant 7KB-0017A (to J.M). K.P.C is an investigator of the Howard Hughes Medical Institute. M.J.B. is a recipient of an Innovator award from the Department of Defense Breast Cancer Research Program and a Distinguished Medical Science Fellow of the Office of Biological and Environmental Research of the Department of Energy.

Abbreviations

BM basement membrane; DG dystroglycan; ECM extracellular matrix; LG laminin G-like; MEC mammary epithelial cell

References

Aumailley, M., Bruckner-Tuderman, L., Carter, W. G., Deutzmann, R., Edgar, D., Ekblom, P., Engel, J., Engvall, E., Hohenester, E., Jones, J. C. et al. (2005). A simplified laminin nomenclature. *Matrix Biol*.

Bissell, M. J., Rizki, A. and Mian, I. S. (2003). Tissue architecture: the ultimate regulator of breast epithelial function. *Curr Opin Cell Biol* **15**, 753-62.

Cohn, R. D., Henry, M. D., Michele, D. E., Barresi, R., Saito, F., Moore, S. A., Flanagan, J. D., Skwarchuk, M. W., Robbins, M. E., Mendell, J. R. et al. (2002). Disruption of DAG1 in differentiated skeletal muscle reveals a role for dystroglycan in muscle regeneration. *Cell* **110**, 639-48.

Colognato, H., Winkelmann, D. A. and Yurchenco, P. D. (1999). Laminin polymerization induces a receptor-cytoskeleton network. *J Cell Biol* **145**, 619-31.

Deng, W. M., Schneider, M., Frock, R., Castillejo-Lopez, C., Gaman, E. A., Baumgartner, S. and Ruohola-Baker, H. (2003). Dystroglycan is required for polarizing the epithelial cells and the oocyte in Drosophila. *Development* **130**, 173-184.

Driss, A., Charrier, L., Yan, Y., Nduati, V., Sitaraman, S. and Merlin, D. (2005). Dystroglycan Receptor Is Involved in Integrin Activation in Intestinal Epithelia. *Am J Physiol Gastrointest Liver Physiol*.

Durbeej, M. and Campbell, K. P. (2002). Muscular dystrophies involving the dystrophin-glycoprotein complex: an overview of current mouse models. *Curr Opin Genet Dev* **12**, 349-61.

Durbeej, M., Henry, M. D., Ferletta, M., Campbell, K. P. and Ekblom, P. (1998). Distribution of dystroglycan in normal adult mouse tissues. *J Histochem Cytochem* **46**, 449-57.

Durbeej, M., Larsson, E., Ibraghimov, B. O., Roberds, S. L., Campbell, K. P. and Ekblom, P. (1995). Non-muscle alpha-dystroglycan is involved in epithelial development. *J Cell Biol* **130**, 79-91.

Durbeej, M., Talts, J. F., Henry, M. D., Yurchenco, P. D., Campbell, K. P. and Ekblom, P. (2001). Dystroglycan binding to laminin alpha1LG4 module influences epithelial morphogenesis of salivary gland and lung in vitro. *Differentiation* **69**, 121-34.

Ervasti, J. M. and Campbell, K. P. (1991). Membrane organization of the dystrophin-glycoprotein complex. *Cell* **66**, 1121-31.

Ervasti, J. M. and Campbell, K. P. (1993). A role for the dystrophin-glycoprotein complex as a transmembrane linker between laminin and actin. *J Cell Biol* **122**, 809-23.

Faraldo, M. M., Deugnier, M. A., Lukashev, M., Thiery, J. P. and Glukhova, M. A. (1998). Perturbation of beta1-integrin function alters the development of murine mammary gland. *Embo J* **17**, 2139-47.

Gee, S. H., Blacher, R. W., Douville, P. J., Provost, P. R., Yurchenco, P. D. and Carbonetto, S. (1993). Laminin-binding protein 120 from brain is closely related to the dystrophin-associated glycoprotein, dystroglycan, and binds with high affinity to the major heparin binding domain of laminin. *J Biol Chem* **268**, 14972-80.

Gudjonsson, T., Ronnov-Jessen, L., Villadsen, R., Rank, F., Bissell, M. J. and Petersen, O. W. (2002). Normal and tumor-derived myoepithelial cells differ in their

ability to interact with luminal breast epithelial cells for polarity and basement membrane deposition. *J Cell Sci* **115**, 39-50.

Henry, M. D. and Campbell, K. P. (1998). A role for dystroglycan in basement membrane assembly. *Cell* **95**, 859-70.

Henry, M. D., Cohen, M. B. and Campbell, K. P. (2001a). Reduced expression of dystroglycan in breast and prostate cancer. *Hum Pathol* **32**, 791-5.

Henry, M. D., Satz, J. S., Brakebusch, C., Costell, M., Gustafsson, E., Fassler, R. and Campbell, K. P. (2001b). Distinct roles for dystroglycan, (&bgr;)1 integrin and perlecan in cell surface laminin organization. *J Cell Sci* **114**, 1137-44.

Ibraghimov-Beskrovnaya, O., Ervasti, J. M., Leveille, C. J., Slaughter, C. A., Sernett, S. W. and Campbell, K. P. (1992). Primary structure of dystrophin-associated glycoproteins linking dystrophin to the extracellular matrix. *Nature* **355**, 696-702.

Ilsley, J. L., Sudol, M. and Winder, S. J. (2002). The WW domain: linking cell signalling to the membrane cytoskeleton. *Cell Signal* **14**, 183-9.

Kaetzel, C. S. and Ray, D. B. (1984). Immunochemical characterization with monoclonal antibodies of three major caseins and alpha-lactalbumin from rat milk. *J Dairy Sci* **67**, 64-75.

Kemler, R., Brulet, P., Schnebelen, M. T., Gaillard, J. and Jacob, F. (1981). Reactivity of monoclonal antibodies against intermediate filament proteins during embryonic development. *J Embryol Exp Morphol* **64**, 45-60.

Kinoshita, S., Su, L., Amano, M., Timmerman, L. A., Kaneshima, H. and Nolan, G. P. (1997). The T cell activation factor NF-ATc positively regulates HIV-1 replication and gene expression in T cells. *Immunity* **6**, 235-44.

Kittrell, F. S., Oborn, C. J. and Medina, D. (1992). Development of mammary preneoplasias in vivo from mouse mammary epithelial cell lines in vitro. *Cancer Research* **52**, 1924-32.

Li, S., Edgar, D., Fassler, R., Wadsworth, W. and Yurchenco, P. D. (2003). The role of laminin in embryonic cell polarization and tissue organization. *Dev Cell* **4**, 613-24.

Li, S., Harrison, D., Carbonetto, S., Fassler, R., Smyth, N., Edgar, D. and Yurchenco, P. D. (2002). Matrix assembly, regulation, and survival functions of laminin and its receptors in embryonic stem cell differentiation. *J Cell Biol* **157**, 1279-90.

Li, S., Liquari, P., McKee, K. K., Harrison, D., Patel, R., Lee, S. and Yurchenco, P. D. (2005). Laminin-sulfatide binding initiates basement membrane assembly and enables receptor signaling in Schwann cells and fibroblasts. *J Cell Biol* **169**, 179-89.

Lohikangas, L., Gullberg, D. and Johansson, S. (2001). Assembly of Laminin Polymers Is Dependent on beta1-Integrins. *Exp Cell Res* **265**, 135-44.

Losasso, C., Di Tommaso, F., Sgambato, A., Ardito, R., Cittadini, A., Giardina, B., Petrucci, T. C. and Brancaccio, A. (2000). Anomalous dystroglycan in carcinoma cell lines. *FEBS Lett* **484**, 194-8.

Michele, D. E., Barresi, R., Kanagawa, M., Saito, F., Cohn, R. D., Satz, J. S., Dollar, J., Nishino, I., Kelley, R. I., Somer, H. et al. (2002). Post-translational disruption of dystroglycan-ligand interactions in congenital muscular dystrophies. *Nature* **418**, 417-22.

Michele, D. E. and Campbell, K. P. (2003). Dystrophin-glycoprotein complex: Post-translational processing and dystroglycan function. *J Biol Chem* **278**, 15457-60.

Miner, J. H. and Yurchenco, P. D. (2004). Laminin Functions in Tissue Morphogenesis. *Annu Rev Cell Dev Biol*.

Moore, S. A., Saito, F., Chen, J., Michele, D. E., Henry, M. D., Messing, A., Cohn, R. D., Ross-Barta, S. E., Westra, S., Williamson, R. A. et al. (2002). Deletion of brain dystroglycan recapitulates aspects of congenital muscular dystrophy. *Nature* **418**, 422-5.

Moss, M. L., Jin, S. L., Milla, M. E., Bickett, D. M., Burkhart, W., Carter, H. L., Chen, W. J., Clay, W. C., Didsbury, J. R., Hassler, D. et al. (1997). Cloning of a disintegrin metalloproteinase that processes precursor tumour-necrosis factor-alpha. *Nature* **385**, 733-6.

Muschler, J., Levy, D., Boudreau, R., Henry, M., Campbell, K. and Bissell, M. J. (2002). A Role for Dystroglycan in Epithelial Polarization: Loss of Function in Breast Tumor Cells. *Cancer Res* **62**, 7102-7109.

Muschler, J., Lochter, A., Roskelley, C. D., Yurchenco, P. and Bissell, M. J. (1999). Division of labor among the alpha6beta4 integrin, beta1 integrins, and an E3 laminin receptor to signal morphogenesis and beta-casein expression in mammary epithelial cells. *Mol Biol Cell* **10**, 2817-28.

Patarroyo, M., Tryggvason, K. and Virtanen, I. (2002). Laminin isoforms in tumor invasion, angiogenesis and metastasis. *Semin Cancer Biol* **12**, 197-207.

Pawson, T. (2004). Specificity in signal transduction: from phosphotyrosine-SH2 domain interactions to complex cellular systems. *Cell* **116**, 191-203.

Peterson, G. L. (1977). A simplification of the protein assay method of Lowry et al. which is more generally applicable. *Anal Biochem* **83**, 346-56.

Sambrook, J., Fritsch, E. F. and Maniatis, T. (1989). Molecular cloning : a laboratory manual. Cold Spring Harbor, N.Y.: Cold Spring Harbor Laboratory.

Scheele, S., Falk, M., Franzen, A., Ellin, F., Ferletta, M., Lonaio, P., Andersson, B., Timpl, R., Forsberg, E. and Ekblom, P. (2005). Laminin alpha1 globular domains 4-5 induce fetal development but are not vital for embryonic basement membrane assembly. *Proc Natl Acad Sci U S A* **102**, 1502-6.

Sgambato, A., Migaldi, M., Montanari, M., Camerini, A., Brancaccio, A., Rossi, G., Cangiano, R., Losasso, C., Capelli, G., Trentini, G. P. et al. (2003). Dystroglycan Expression Is Frequently Reduced in Human Breast and Colon Cancers and Is Associated with Tumor Progression. *Am J Pathol* **162**, 849-860.

Singh, J., Itahana, Y., Knight-Krajewski, S., Kanagawa, M., Campbell, K. P., Bissell, M. J. and Muschler, J. (2004). Proteolytic enzymes and altered glycosylation modulate dystroglycan function in carcinoma cells. *Cancer Res* **64**, 6152-9.

Slade, M. J., Coope, R. C., Gomm, J. J. and Coombes, R. C. (1999). The human mammary gland basement membrane is integral to the polarity of luminal epithelial cells. *Exp Cell Res* **247**, 267-78.

Sotgia, F., Lee, H., Bedford, M. T., Petrucci, T., Sudol, M. and Lisanti, M. P. (2001). Tyrosine phosphorylation of beta-dystroglycan at its WW domain binding motif, PPxY, recruits SH2 domain containing proteins. *Biochemistry* **40**, 14585-92.

Streuli, C. H., Bailey, N. and Bissell, M. J. (1991). Control of mammary epithelial differentiation: basement membrane induces tissue-specific gene expression in the absence of cell-cell interaction and morphological polarity. *J Cell Biol* **115**, 1383-95.

Streuli, C. H., Schmidhauser, C., Bailey, N., Yurchenco, P., Skubitz, A. P., Roskelley, C. and Bissell, M. J. (1995). Laminin mediates tissue-specific gene expression in mammary epithelia. *J Cell Biol* **129**, 591-603.

Weaver, V. M., Petersen, O. W., Wang, F., Larabell, C. A., Briand, P., Damsky, C. and Bissell, M. J. (1997). Reversion of the malignant phenotype of human breast cells in three- dimensional culture and in vivo by integrin blocking antibodies. *J Cell Biol* **137**, 231-45.

Weir, M. L. and Muschler, J. (2003). Dystroglycan: emerging roles in mammary gland function. *J Mammary Gland Biol Neoplasia* **8**, 409-19.

Williamson, R. A., Henry, M. D., Daniels, K. J., Hrstka, R. F., Lee, J. C., Sunada, Y., Ibraghimov, B. O. and Campbell, K. P. (1997). Dystroglycan is essential for early embryonic development: disruption of Reichert's membrane in Dag1-null mice. *Hum Mol Genet* **6**, 831-41.

Yang, B., Jung, D., Motto, D., Meyer, J., Koretzky, G. and Campbell, K. P. (1995). SH3 domain-mediated interaction of dystroglycan and Grb2. *J Biol Chem* **270**, 11711-4.

Yeaman, C., Grindstaff, K. K. and Nelson, W. J. (1999). New perspectives on mechanisms involved in generating epithelial cell polarity. *Physiol Rev* **79**, 73-98.

FIGURE LEGENDS

Figure 1. **Generation of DG+/+ and partial DG-/- MEC populations by adenoviral infection of immortalized mouse MECs.** A) Diagram of DG, including the extracellular α-DG subunit, with central mucin domain, and the transmembrane β-DG subunit. B) Diagram of laminin-111 (LN), including the 3 subunits (α, β, γ), and the 5 C-terminal LG domains, with respective receptor binding sites. C) Western blot of cell extracts (5 μg protein) prepared on various days after infection of immortalized floxed DG mouse MEpG cell line with control or Cre recombinase-expressing adenovirus to generate DG+/+ and partial DG-/- cell populations, respectively. Lane 1 represents uninfected cells at time 0. Blots were incubated with antibodies specific for α-DG, C-terminal β-DG, or E-cadherin (loading control), followed by HRP-conjugated secondary antibodies. Sizes of molecular weight markers are shown in kDa. D) Vertically paired immunofluorescent images of DG+/+ and partial DG-/- cell populations using primary antibodies specific for α-DG or C-terminal β-DG, followed by FITC-labeled secondary antibodies (upper panel). Nuclei were stained with propidium iodide (bottom panel). Bar, 60 μm.

Figure 2. **Loss of polarity in DG-/- colonies grown in a 3-D matrix of collagen I/laminin-111.** DG+/+ and DG-/- cells were grown in a 3-D matrix of collagen I or collagen I/laminin-111 and co-immunostained. Confocal immunofluorescent images were taken at colony centers. Bar, 10 μm. A) Staining using ZO-1 and α6 integrin antibodies, visualized with FITC- (green) and Cy-5- (blue) labeled secondary antibodies, respectively, and propidium iodide to stain nuclei (red). B) Staining using α6 integrin and C-terminal β-DG (insets) antibodies, detected with rhodamine- (red) and Cy-5- (blue changed to white for easier visualization) labeled secondary antibodies, respectively. Actin was seen using Alexa Fluor 488 phalloidin (green). Overlap between actin and α6 integrin staining appeared yellow. C) Quantification of polarity in DG+/+ and DG-/- colonies grown in collagen I (C) or collagen I/laminin-111 (C/L) using ZO-1 as a polarity marker. Results are shown as the average $\pm$ SEM of 4-6 independent experiments, each with triplicate or quadruplicate counts. * $P<0.01$ for all paired combinations.

Figure 3. **Loss of laminin binding and DG co-localization on the surface of DG-/- cells grown in a 3-D matrix of collagen I or collagen I/laminin-111.** A) Vertically paired confocal immunofluorescent images of DG+/+ and DG-/- cells grown in collagen I or collagen I/laminin-111. Samples were co-immunostained with laminin, α6 integrin, and C-terminal β-DG (insets) antibodies, followed by rhodamine- (red), FITC- (green), and Cy-5- (blue changed to white for easier visualization) labelled secondary antibodies, respectively. Images were taken at colony centers. B) Confocal immunofluorescent images taken at the cell surface of DG+/+ colonies shown in A to reveal co-staining for laminin, β-DG, and their extent of co-localization. Arrows point to polygonal arrays of laminin. Bar, 10 μm.

Figure 4. **DG-/- cell monolayers failed to bind endogenous laminin or exogenous laminin-111-FITC.** A) Vertically paired immunofluorescent images of DG+/+ and

partial DG-/- cell populations co-stained using laminin and C-terminal β-DG antibodies, followed by rhodamine- and FITC-labelled secondary antibodies, respectively, all in the presence of Tween-20 (images above line). Arrows point to a DG-/- cell that retained staining for intracellular, but not cell surface, laminin. Cells immunostained for laminin in the absence of Tween-20 are shown below the line, with corresponding phase images. B) Immunofluorescent images of DG+/+ and partial DG-/- cell populations treated with 10 nM exogenously added laminin-111-FITC for 4 h. Samples were co-stained using C-terminal β-DG antibody and rhodamine-labelled secondary antibody. Corresponding phase images are shown in the bottom panel. Arrows point to a DG-/- cell lacking laminin-111-FITC staining. C) Immunofluorescent images of DG+/+ cells treated with 10 nM exogenous laminin-111-FITC for 24 h in the absence or presence of α6 and/or β1 integrin function blocking antibodies (upper panel). Corresponding phase images are shown in the bottom panel. Insets show cells incubated only with 10 nM AEBSF-treated laminin-111 for 24 h, followed by immunostaining for laminin as described for upper images in A. Bars, 10 μm.

Figure 5. **Partial DG+/+ colonies grown in a 3-D matrix of collagen I/laminin-111 retain laminin and DG co-localization on the surface of DG +/+ cells only, but fail to polarize.** A) and B) Confocal immunofluorescent images taken at the center of partial DG+/+ colonies grown in collagen I/laminin-111 and co-immunostained as follows: A) α6 integrin and C-terminal β-DG antibodies were detected using rhodamine- (red) and Cy-5- (blue) labelled secondary antibodies, respectively. Actin was visualized with Alexa Fluor 488 phalloidin (green). B) Laminin, α6 integrin, and C-terminal β-DG antibodies were detected using rhodamine- (red), FITC- (green), and Cy-5- (blue) labelled secondary antibodies, respectively. Arrows show part of colony surface lacking laminin and β-DG staining. C) Confocal immunofluorescent images were taken at the cell surface of the colony shown in B to reveal co-staining for laminin, β-DG, and their extent of co-localization. Dotted outline represents outer edge of colony. Bar, 10 μm.

Figure 6. **Loss of β-casein production in response to laminin-111 in DG-/- cells.** A) Western blot of cell extracts (10 μg protein) prepared from DG+/+ and partial DG-/- cell population incubated with laminin-111 overlay in the absence (-) or presence (+) of prolactin and hydrocortisone. Blots were incubated with antibodies specific for β-casein or E-cadherin (loading control), followed by HRP-conjugated secondary antibodies. Sizes of molecular weight markers are shown in kDa. Dotted lines separate non-adjacent lanes derived from the same blot. B) Immunofluorescent images of DG+/+ and partial DG-/- cell population treated with 10 nM exogenously added laminin-111-FITC for 4 h. Samples were co-stained using C-terminal β-DG antibody and rhodamine-labelled secondary antibody. Corresponding phase images are shown in the bottom panel. Arrows point to a DG-/- cell lacking laminin-111-FITC binding. Bar, 10 μm.

Figure 7. **Re-expression of full length DG or DG mutants in a completely DG-/- cell line restored laminin-111 binding on monolayer cell surfaces.** A) Western blot of cell extracts (10 μg protein) prepared from DG+/+ cells and a completely DG-/- cell line (derived from MEpG cells) infected with retroviral vector (VEC) or that encoding full

length DG (wtDG) or various β-DG cytoplasmic deletions (DEL A, B, C). Blots were incubated with antibodies specific for α-DG, N-terminal β-DG (right panel), C-terminal β-DG (left panel), or E-cadherin (loading control), followed by HRP-conjugated secondary antibodies. Sizes of molecular weight markers are shown in kDa. B) Paired immunofluorescent images of cells in A, co-stained for α-DG and nuclei, using FITC-labelled secondary antibody and propidium iodide, respectively. C) Immunofluorescent images of cells in A, treated for 4 h with 10 nM exogenously added laminin-111-FITC. Corresponding phase images are shown in the bottom panel. Bar, 10 μm.

Figure 8. **Expression of full length DG and DG mutants in a completely DG-/- cell line restored polarity and surface laminin in a 3-D matrix of collagen I/laminin-111.** A) Confocal immunofluorescent images taken at the center of colonies grown in collagen I (upper panel) or collagen I/laminin-111 (middle panel). Samples were co-stained for ZO-1, α6 integrin, and nuclei as described in Fig. 2A. Bottom panel shows laminin staining of a second group of colonies grown in collagen I/laminin-111, visualized with rhodamine-labeled secondary antibody (red). Cells are described in Fig. 7A. Bar, 10 μm. B) Quantification of polarity in colonies grown in collagen I (C) or collagen I/laminin-111 (C/L) using ZO-1 as a polarity marker. Results are shown as the average $\pm$ SEM of 3-5 independent experiments, each with triplicate or quadruplicate counts. (^) or (*) = $P<0.001$ for all paired combinations except with each other.

Figure 9. **Expression of full length DG and DG mutants in a completely DG-/- cell line restored β-casein protein expression in response to laminin-111.** Western blot of cell extracts prepared from cells infected with retroviral vector (VEC) or that encoding full length DG (wtDG) or various β-DG cytoplasmic deletions (DEL A, B, C) and incubated with a laminin-111 overlay in the absence (-) or presence (+) of prolactin and hydrocortisone. Blots were incubated with antibodies specific for β-casein or E-cadherin (loading control), followed by HRP-conjugated secondary antibodies. Sizes of molecular weight markers are shown in kDa.

Figure 10. **The DG extracellular domain alone is critical to laminin assembly.** A) Western blot of cell extracts prepared from a completely DG-/- cell line (derived from MEpL cells) infected with retroviral vector (VEC) or that encoding full length DG (wtDG), a fusion protein comprised of the extracellular DG sequences fused to the transmembrane region of TACE (DG-tmf), or deletions within the α-DG mucin domain (DEL D, E). Blots were incubated with antibodies specific for α-DG, N-terminal β-DG, or E-cadherin (loading control). Sizes of molecular weight markers are shown in kDa. B) Immunofluorescent images of cells in A, treated for 4 h with 10 nM exogenously added laminin-111-FITC. Corresponding phase images are shown in the bottom panel. Bar, 10 μm.

Figure 11. **Model for DG's role as a MEC co-receptor in laminin-111 assembly and laminin-111-induced functions.** α-DG on the MEC surface serves as the initial anchoring site for laminin-111 (LN) monomers by interacting with their C-terminal LG domains (step 1). The laminin-111/DG complexes recruit β1 integrin (INT) co-receptors,

which contribute to laminin-111 polymerization (step 2). Subsequent activation of co-receptors, possibly integrins (INT), influences intracellular signaling pathways leading to polarity and β-casein induction (step 3).

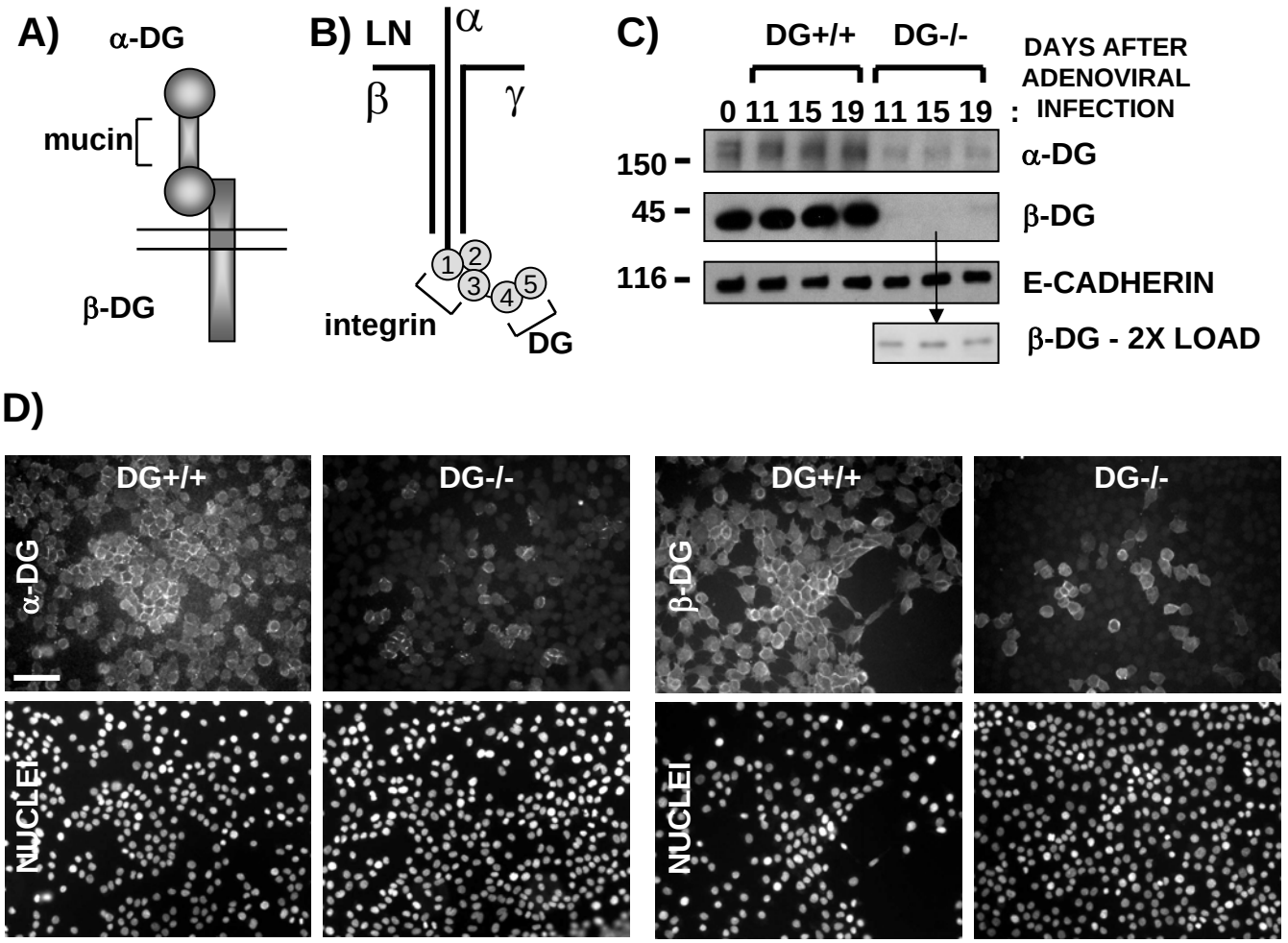

Figure 1. **Generation of DG+/+ and partial DG-/- MEC populations by adenoviral infection of immortalized mouse MECs.** A) Diagram of DG, including the extracellular α-DG subunit, with central mucin domain, and the transmembrane β-DG subunit. B) Diagram of laminin-111 (LN), including the 3 subunits (α, β, γ), and the 5 C-terminal LG domains, with respective receptor binding sites. C) Western blot of cell extracts (5 ug protein) prepared on various days after infection of immortalized floxed DG mouse MEpG cell line with control or Cre recombinase-expressing adenovirus to generate DG+/+ and partial DG-/- cell populations, respectively. Lane 1 represents uninfected cells at time 0. Blots were incubated with antibodies specific for α-DG, C-terminal β-DG, or E-cadherin (loading control), followed by HRP-conjugated secondary antibodies. Sizes of molecular weight markers are shown in kDa. D) Vertically paired immunofluorescent images of DG+/+ and partial DG-/- cell populations using primary antibodies specific for α-DG or C-terminal β-DG, followed by FITC-labeled secondary antibodies (upper panel). Nuclei were stained with propidium iodide (bottom panel). Bar, 60 um.

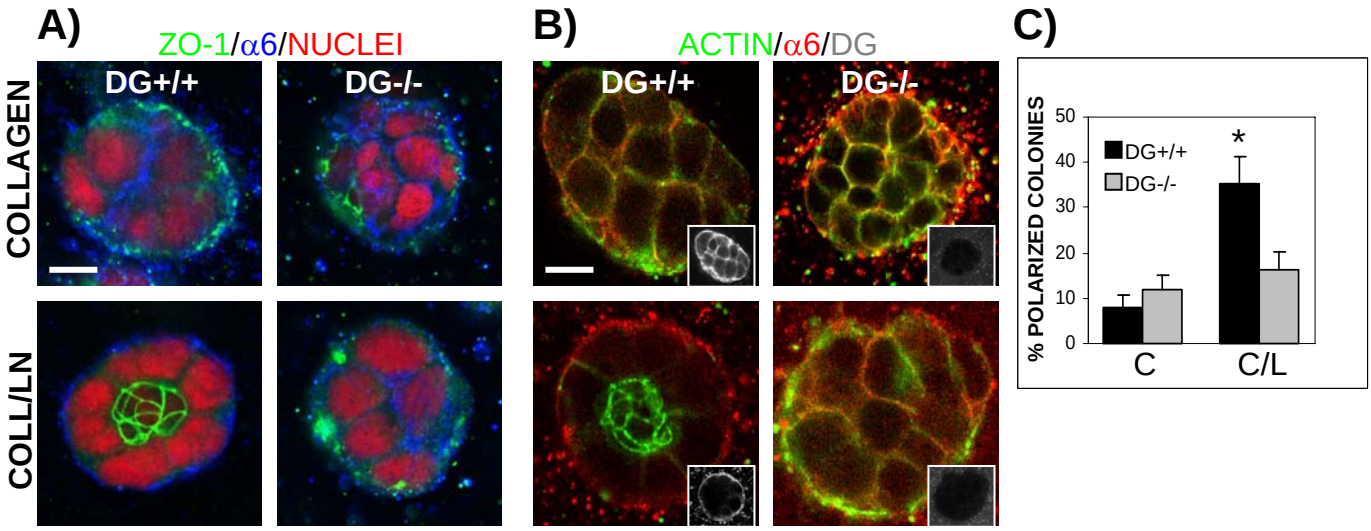

Figure 2. **Loss of polarity in DG-/- colonies grown in a 3-D matrix of collagen I/laminin-1.** DG+/+ and DG-/- cells were grown in a 3-D matrix of collagen I or collagen I/laminin-111 and co-immunostained. Confocal immunofluorescent images were taken at colony centers. Bar, 10 um. A) Staining using ZO-1 and α6 integrin antibodies, visualized with FITC- (green) and Cy-5- (blue) labeled secondary antibodies, respectively, and propidium iodide to stain nuclei (red). B) Staining using α6 integrin and C-terminal β-DG (insets) antibodies, detected with rhodamine- (red) and Cy-5- (blue changed to white for easier visualization) labeled secondary antibodies, respectively. Actin was seen using Alexa Fluor 488 phalloidin (green). Overlap between actin and α6 integrin staining appeared yellow. C) Quantification of polarity in DG+/+ and DG-/- colonies grown in collagen I (C) or collagen I/laminin-111 (C/L) using ZO-1 as a polarity marker. Results are shown as the average ± SEM of 4-6 independent experiments, each with triplicate or quadruplicate counts. * $P<0.01$ for all paired combinations.

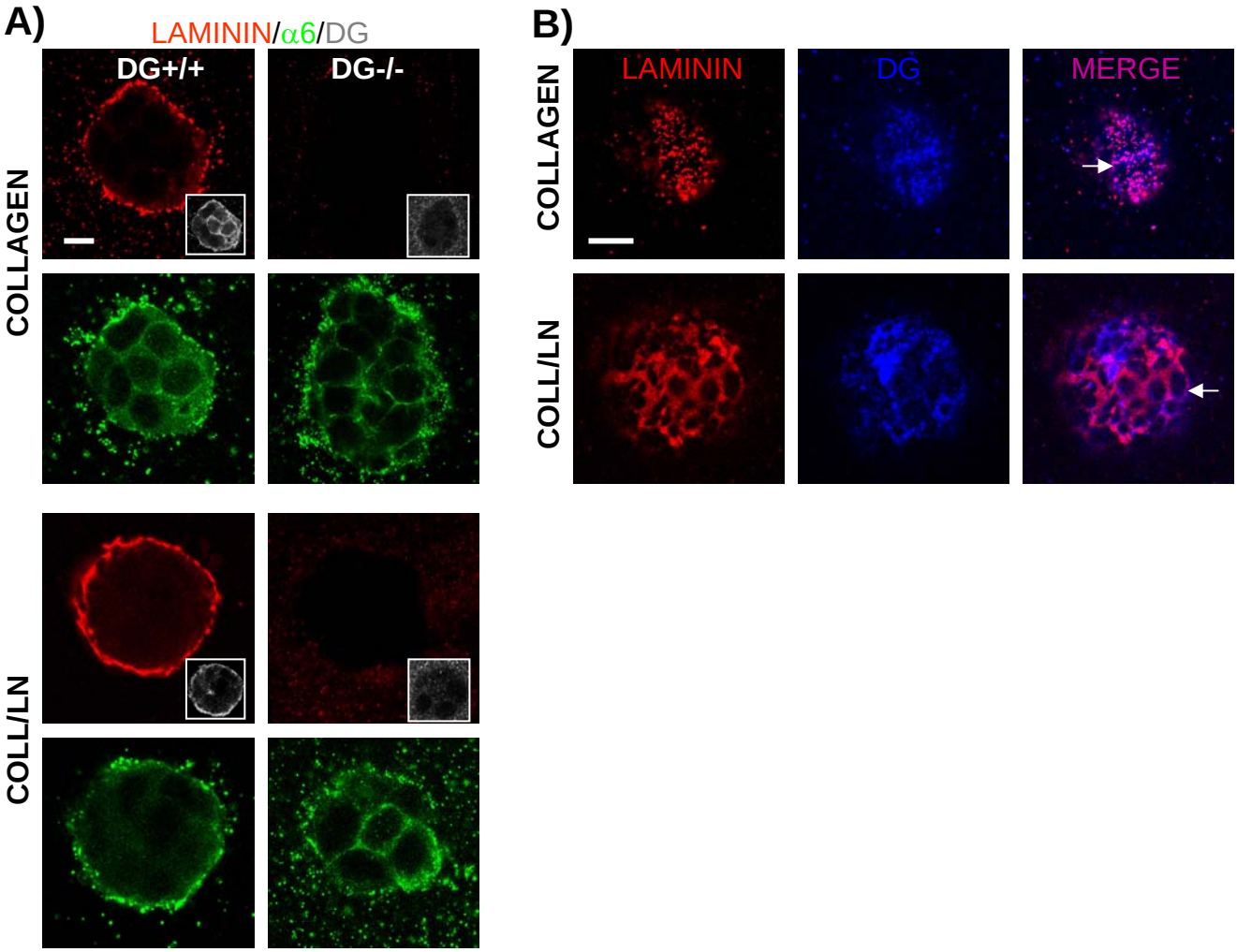

Figure 3. **Loss of laminin binding and DG co-localization on the surface of DG-/- cells grown in a 3-D matrix of collagen I or collagen I/laminin-111.** A) Vertically paired confocal immunofluorescent images of DG+/+ and DG-/- cells grown in collagen I or collagen I/laminin-111. Samples were co-immunostained with laminin, α6 integrin, and C-terminal β-DG (insets) antibodies, followed by rhodamine- (red), FITC- (green), and Cy-5- (blue changed to white for easier visualization) labelled secondary antibodies, respectively. Images were taken at colony centers. B) Confocal immunofluorescent images taken at the cell surface of DG+/+ colonies shown in A to reveal co-staining for laminin, β-DG, and their extent of co-localization. Arrows point to polygonal arrays of laminin. Bar, 10 um.

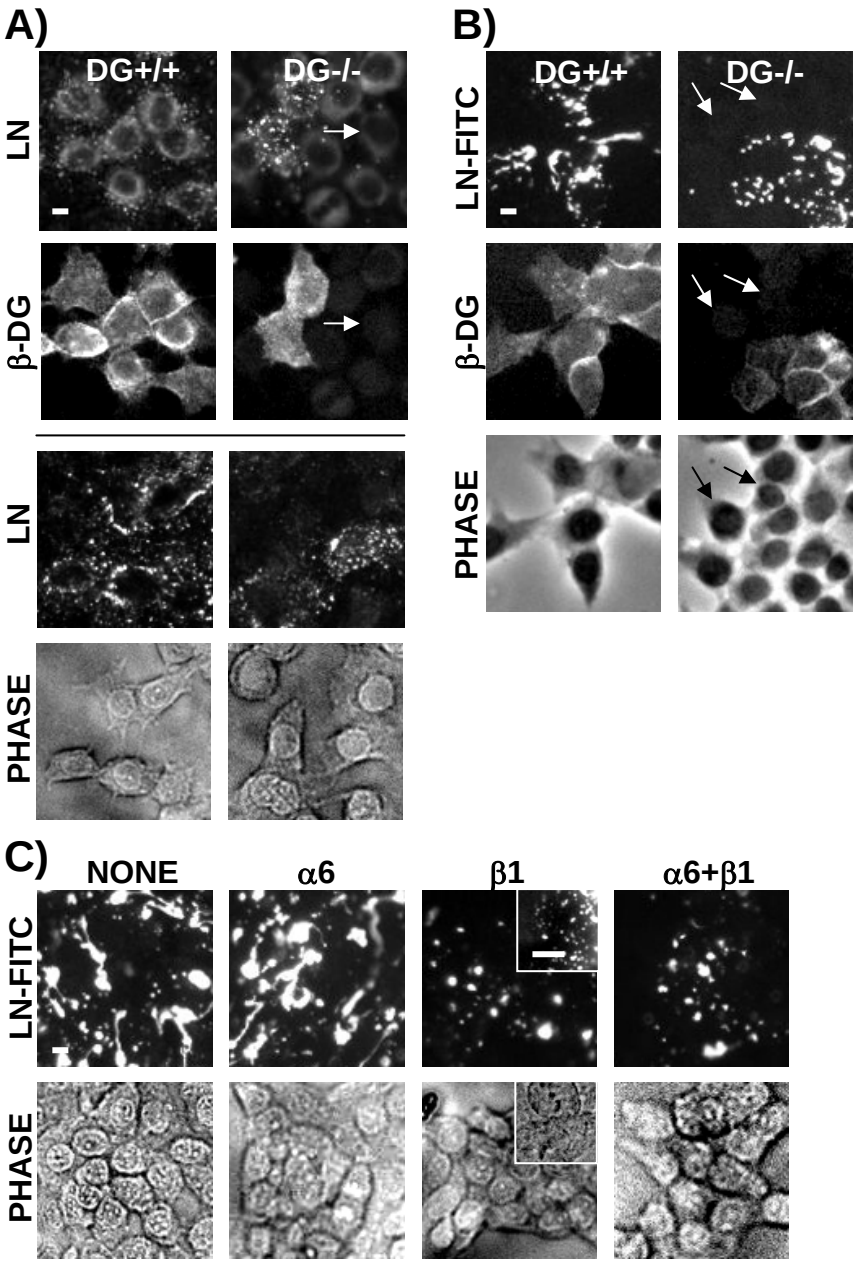

Figure 4. **DG-/- cell monolayers failed to bind endogenous laminin or exogenous laminin-111-FITC.** A) Vertically paired immunofluorescent images of DG+/+ and partial DG-/- cell populations co-stained using laminin and C-terminal β-DG antibodies, followed by rhodamine- and FITC-labelled secondary antibodies, respectively, all in the presence of Tween-20 (images above line). Arrows point to a DG-/- cell that retained staining for intracellular, but not cell surface, laminin. Cells immunostained for laminin in the absence of Tween-20 are shown below the line, with corresponding phase images. B) Immunofluorescent images of DG+/+ and partial DG-/- cell populations treated with 10 nM exogenously added laminin-111-FITC for 4 h. Samples were co-stained using C-terminal β-DG antibody and rhodamine-labelled secondary antibody. Corresponding phase images are shown in the bottom panel. Arrows point to a DG-/- cell lacking laminin-111-FITC staining. C) Immunofluorescent images of DG+/+ cells treated with 10 nM exogenous laminin-111-FITC for 24 h in the absence or presence of α6 and/or β1 integrin function blocking antibodies (upper panel). Corresponding phase images are shown in the bottom panel. Insets show cells incubated only with 10 nM AEBSF-treated laminin-1 for 24 h, followed by immunostaining for laminin as described for upper images in A. Bars, 10 um.

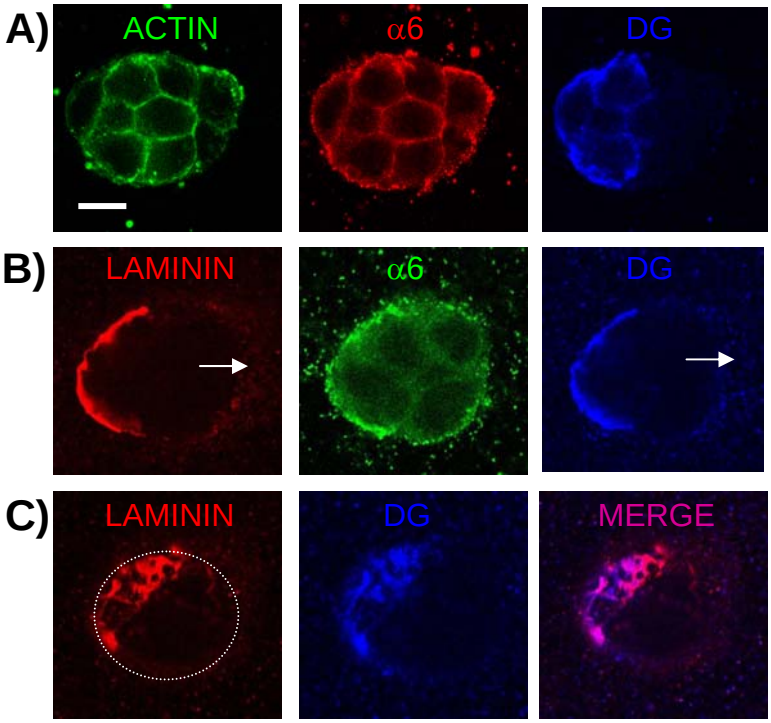

Figure 5. **Partial DG+/+ colonies grown in a 3-D matrix of collagen I/laminin-111 retained laminin and DG co-localization on the surface of DG +/+ cells only, but failed to polarize.** A) and B) Confocal immunofluorescent images taken at the center of partial DG+/+ colonies grown in collagen I/laminin-111 and co-immunostained as follows: A) α6 integrin and C-terminal β-DG antibodies were detected using rhodamine- (red) and Cy-5- (blue) labelled secondary antibodies, respectively. Actin was visualized with Alexa Fluor 488 phalloidin (green). B) Laminin, α6 integrin, and C-terminal β-DG antibodies were detected using rhodamine- (red), FITC- (green), and Cy-5- (blue) labelled secondary antibodies, respectively. Arrows show part of colony surface lacking laminin and β-DG staining. C) Confocal immunofluorescent images were taken at the cell surface of the colony shown in B to reveal co-staining for laminin, β-DG, and their extent of co-localization. Dotted outline represents outer edge of colony. Bar, 10 μm.

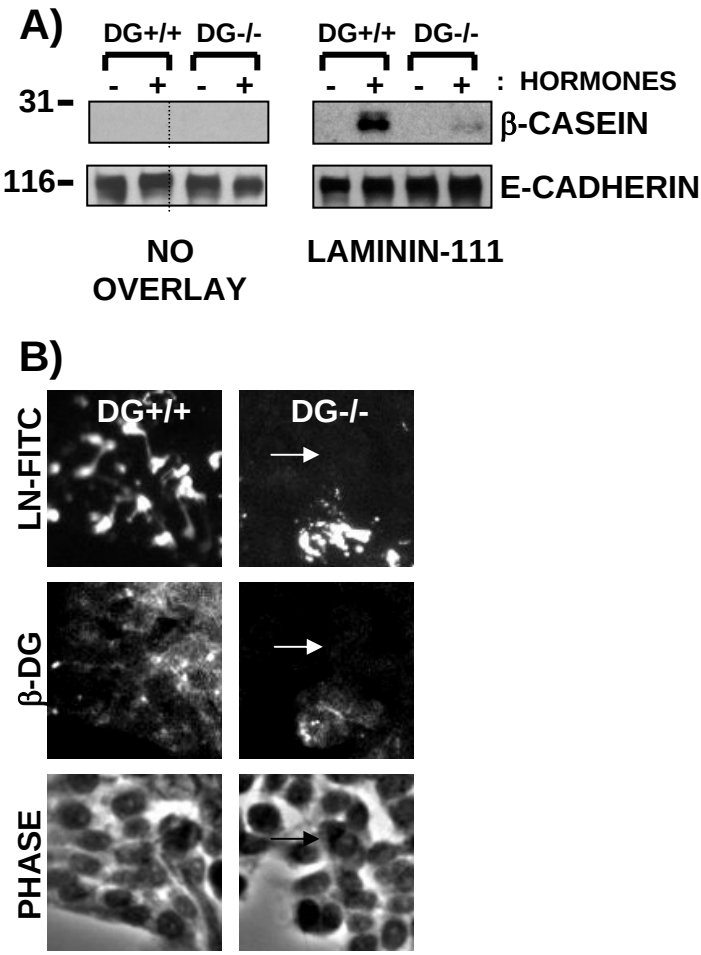

Figure 6. **Loss of β-casein production in response to laminin-111 in DG-/- cells.** A) Western blot of cell extracts (10 μg protein) prepared from DG+/+ and partial DG-/- cell population incubated without or with laminin-111 overlay in the absence (-) or presence (+) of prolactin and hydrocortisone. Blots were incubated with antibodies specific for β-casein or E-cadherin (loading control), followed by HRP-conjugated secondary antibodies. Sizes of molecular weight markers are shown in kDa. Dotted lines separate non-adjacent lanes derived from the same blot. B) Immunofluorescent images of DG+/+ and partial DG-/- cell population treated with 10 nM exogenously added laminin-111-FITC for 4 h. Samples were co-stained using C-terminal β-DG antibody and rhodamine-labelled secondary antibody. Corresponding phase images are shown in the bottom panel. Arrows point to a DG-/- cell lacking laminin-111-FITC binding. Bar, 10 μm.

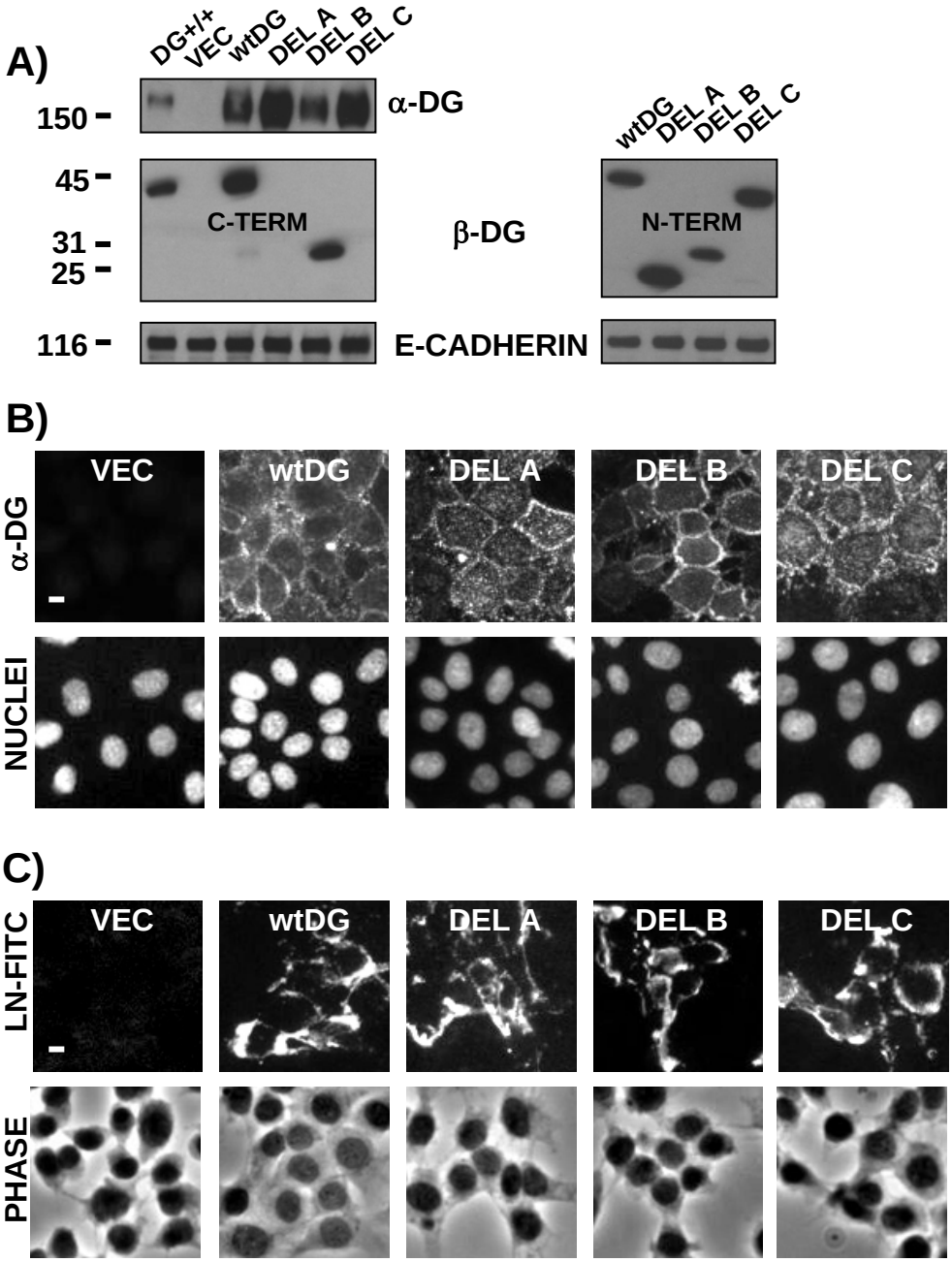

Figure 7. **Re-expression of full length DG or DG mutants in a completely DG-/- cell line restored laminin-111 binding on monolayer cell surfaces.** A) Western blot of cell extracts (10 ug protein) prepared from DG+/+ cells and a completely DG-/- cell line (derived from MEpG cells) infected with retroviral vector (VEC) or that encoding full length DG (wtDG) or various β-DG cytoplasmic deletions (DEL A, B, C). Blots were incubated with antibodies specific for α-DG, N-terminal β-DG (right panel), C-terminal β-DG (left panel), or E-cadherin (loading control), followed by HRP-conjugated secondary antibodies. Sizes of molecular weight markers are shown in kDa. B) Paired immunofluorescent images of cells in A, co-stained for α-DG and nuclei, using FITC-labelled secondary antibody and propidium iodide, respectively. C) Immunofluorescent images of cells in A, treated for 4 h with 10 nM exogenously added laminin-111-FITC. Corresponding phase images are shown in the bottom panel. Bar, 10 um.

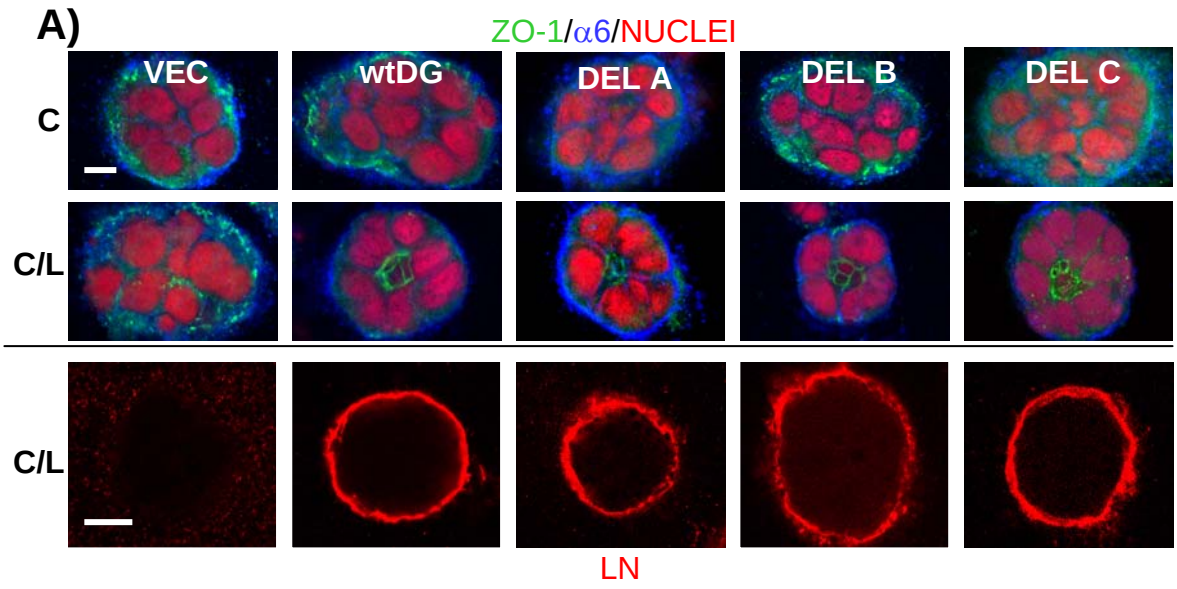

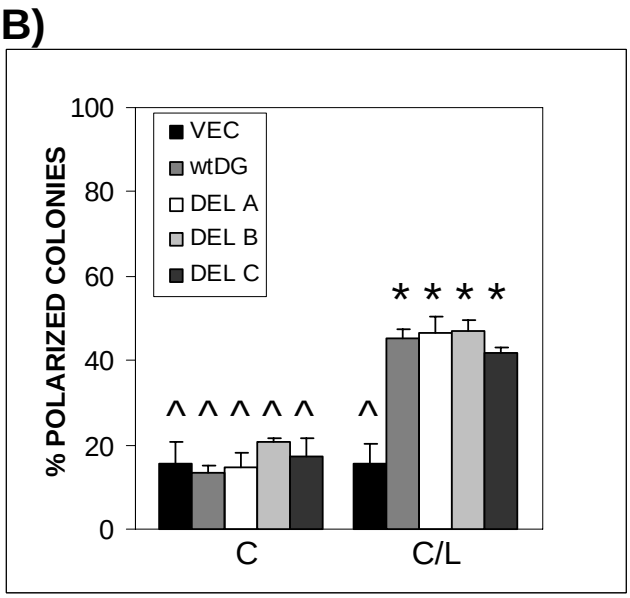

Figure 8. **Expression of full length DG and DG mutants in a completely DG-/- cell line restored polarity and surface laminin in a 3-D matrix of collagen I/laminin-111.** A) Confocal immunofluorescent images taken at the center of colonies grown in collagen I (upper panel) or collagen I/laminin-111 (middle panel). Samples were co-stained for ZO-1, α6 integrin, and nuclei as described in Fig. 2A. Bottom panel shows laminin staining of a second group of colonies grown in collagen I/laminin-111, visualized with rhodamine-labelled secondary antibody (red). Cells are described in Fig. 7A. Bar, 10 um. B) Quantification of polarity in colonies grown in collagen I (C) or collagen I/laminin-111 (C/L) using ZO-1 as a polarity marker. Results are shown as the average $\pm$ SEM of 3-5 independent experiments, each with triplicate or quadruplicate counts. (^) or (*) = $P<0.001$ for all paired combinations except with each other.

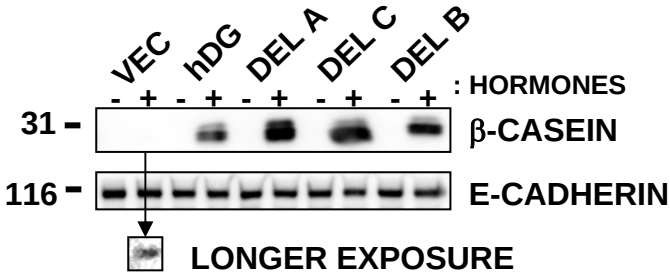

Figure 9. **Expression of full length DG and DG mutants in a completely DG-/- cell line restored β-casein protein expression in response to laminin-111.** Western blot of cell extracts (10 ug protein) prepared from cells infected with retroviral vector (VEC) or that encoding full length DG (wtDG) or various β-DG cytoplasmic deletions (DEL A, B, C) and incubated with a laminin-111 overlay in the absence (-) or presence (+) of prolactin and hydrocortisone. Blots were incubated with antibodies specific for β-casein or E-cadherin (loading control), followed by HRP-conjugated secondary antibodies. Sizes of molecular weight markers are shown in kDa.

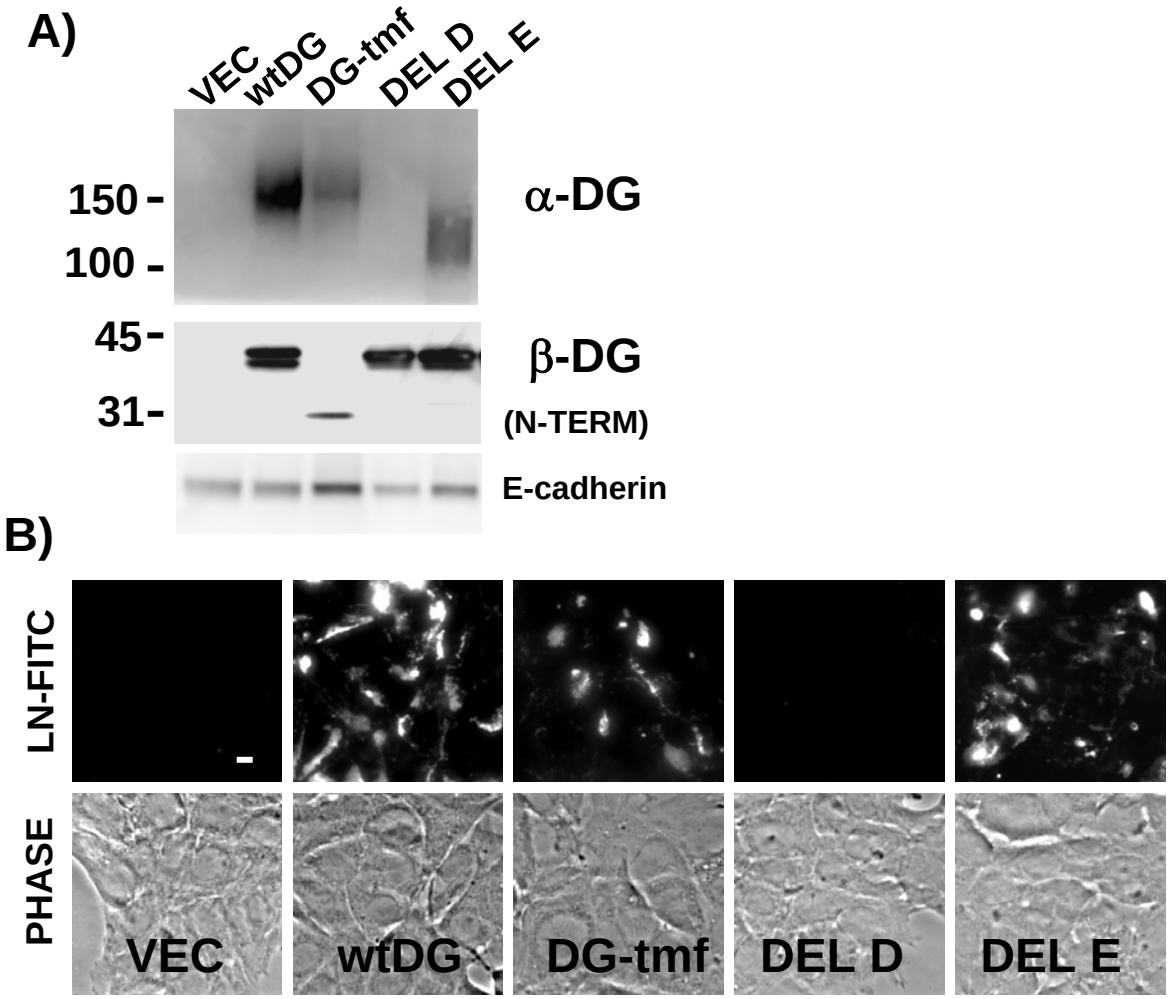

Figure 10. **The DG extracellular domain alone is critical to laminin assembly.** A) Western blot of cell extracts prepared from a completely DG-/- cell line (derived from MEpL cells) infected with retroviral vector (VEC) or that encoding full length DG (wtDG), a fusion protein comprised of the extracellular DG sequences fused to the transmembrane region of TACE (DG-tmf), or deletions within the α-DG mucin domain (DEL D, E). Blots were incubated with antibodies specific for α-DG, N-terminal β-DG, or E-cadherin (loading control). Sizes of molecular weight markers are shown in kDa. B) Immunofluorescent images of cells in A, treated for 4 h with 10 nM exogenously added laminin-111-FITC. Corresponding phase images are shown in the bottom panel. Bar, 10 μm.

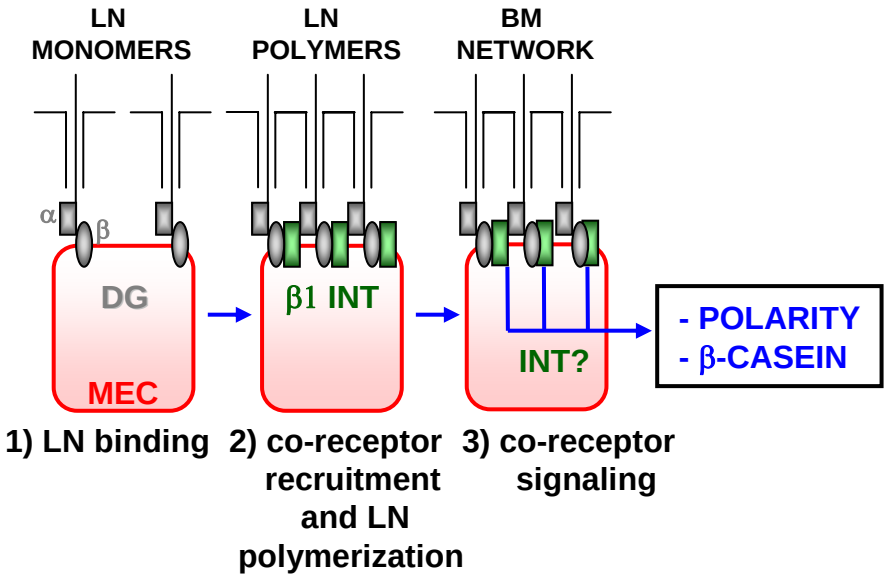

Figure 11. **Model for DG's role as a MEC co-receptor in laminin-111 assembly and laminin-111-induced functions.** α-DG on the MEC surface serves as the initial binding site for laminin-111 (LN) monomers by interacting with their C-terminal LG domains (step 1). The laminin-1/DG complexes recruit β1 integrin (INT) co-receptors, which contribute to laminin-111 polymerization (step 2). Subsequent activation of co-receptors, possibly integrins (INT), influences intracellular signaling pathways leading to polarity and β-casein induction (step 3).

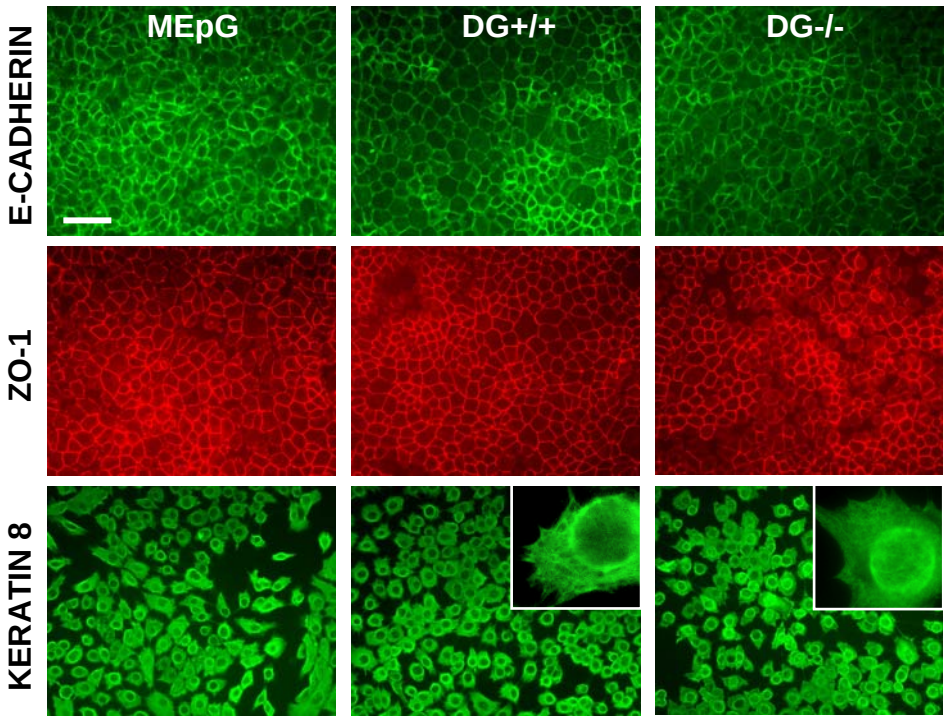

Fig. S1. Established cell lines display epithelial markers before and after adenoviral infection. Monolayers of uninfected MEpG cells (left panel) or those infected with either a control or Cre-expressing adenovirus to generate DG+/+ cells (middle panel) or DG-/- cells (right panel), respectively, were fixed in acetone/methanol and immunostained as described in Materials and methods. Mouse mAb specific for E-cadherin (BD Transduction Labs) was used at 1:200. Rat mAb TROMA-1 specific for keratin 8 was used at 1:30 (obtained from Developmental Studies Hybridoma Bank under the auspices of the NICHD; maintained by University of Iowa, Dept. of Biol. Sciences, Iowa City, IA) (Kemler et al., 1981). Both of the former antibodies were visualized with FITC-conjugated secondary antibodies (green). Rabbit pAb specific for ZO-1 (Zymed) was used at 1:100 and detected with rhodamine-conjugated secondary antibody (red). Images were captured using a Nikon Eclipse E800 microscope, SPOT camera (Diagnostic Instruments Inc), Image-Pro Plus 3.0.01.00 software (Media Cybernetics), and a Nikon Plan Fluor Ph1 DLL 20X objective (0.50 NA). Bar, 60 um.

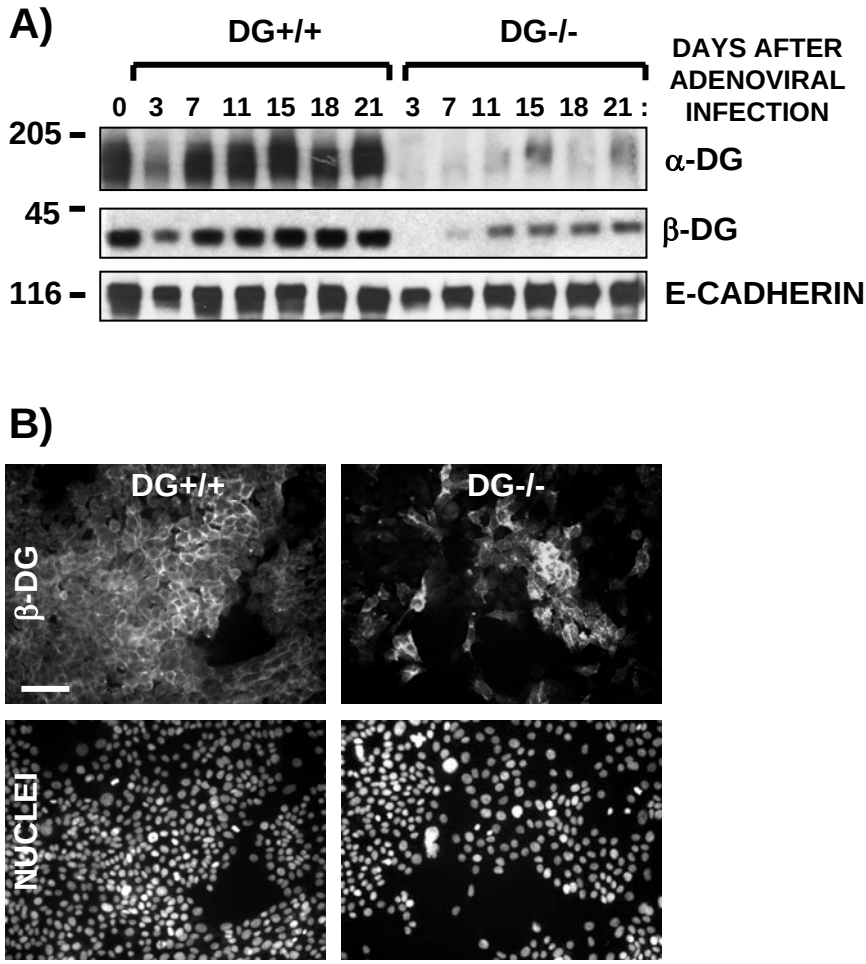

Fig. S2. DG protein levels in DG+/+ and partial DG-/- MEC populations generated by adenoviral infection of the MEpL cell line. Shown in A is a Western blot of cell extracts (10 ug protein) prepared on various days after infection of immortalized floxed DG mouse MEpL cell line with control or Cre recombinase-expressing adenovirus to generate DG+/+ or partial DG-/- cell populations, respectively. Lane 1 represents uninfected cells at time 0. Antibodies are described in the legend for Fig. 1. Sizes of molecular weight markers are given in kDa. Shown in B are vertically paired immunofluorescent images of DG+/+ and partial DG-/- cell populations that were stained using a C-terminal β-DG antibody followed by a FITC-labeled secondary antibody (upper panel). Nuclei were stained with propidium iodide (bottom panel). Bar, 60 um.

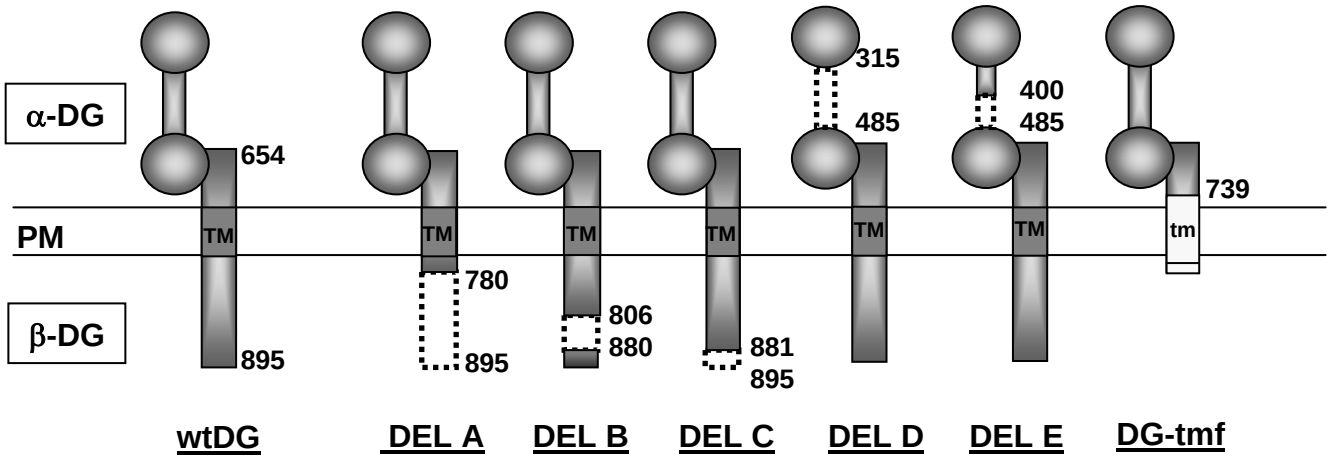

Fig. S3. Diagram of DG mutants. Shown are the structures of full length DG (wtDG), deletion mutants (DEL A, B, C, D, and E) and the transmembrane fusion mutant (DG-tmf), consisting of extracellular DG sequences fused to the transmembrane domain of TACE. Numbers refer to amino acids in human α- and β-DG, with deleted sequences shown by dotted lines. "PM" refers to the plasma membrane."TM" refers to the transmembrane domain of β-DG, and "tm" to the transmembrane domain of TACE.